



**AFRL-RQ-WP-TR-2013-0204**

# **AQUEOUS SOLUTION HEAT PIPE TRANSPORT: QU-TUBE VS. CAPILLARY-PUMPED HEAT PIPE**

**Kenneth D. Kihm**

**The University of Tennessee**

**JULY 2013**

**Final Report**

**Approved for public release; distribution unlimited.**

*See additional restrictions described on inside pages*

**STINFO COPY**

**AIR FORCE RESEARCH LABORATORY  
AEROSPACE SYSTEMS DIRECTORATE  
WRIGHT-PATTERSON AIR FORCE BASE, OH 45433-7542  
AIR FORCE MATERIEL COMMAND  
UNITED STATES AIR FORCE**

## NOTICE AND SIGNATURE PAGE

Using Government drawings, specifications, or other data included in this document for any purpose other than Government procurement does not in any way obligate the U.S. Government. The fact that the Government formulated or supplied the drawings, specifications, or other data does not license the holder or any other person or corporation; or convey any rights or permission to manufacture, use, or sell any patented invention that may relate to them.

This report was cleared for public release by the USAF 88th Air Base Wing (88 ABW) Public Affairs Office (PAO) and is available to the general public, including foreign nationals.

Copies may be obtained from the Defense Technical Information Center (DTIC)  
(<http://www.dtic.mil>).

AFRL-RQ-WP-TR-2013-0204 HAS BEEN REVIEWED AND IS APPROVED FOR  
PUBLICATION IN ACCORDANCE WITH ASSIGNED DISTRIBUTION STATEMENT.

\*//Signature//

---

ANDREW D. SWANSON  
Senior Aerospace Engineer  
Vehicle Technology Branch  
High Speed Systems Division

//Signature//

---

TROY C. HOEGER, Branch Chief  
Vehicle Technology Branch  
High Speed Systems Division

//Signature//

---

THOMAS A. JACKSON  
Deputy for Science  
High Speed Systems Division  
Aerospace Systems Directorate

This report is published in the interest of scientific and technical information exchange, and its publication does not constitute the Government's approval or disapproval of its ideas or findings.

\*Disseminated copies will show “//Signature//” stamped or typed above the signature blocks.

REPORT DOCUMENTATION PAGE					Form Approved OMB No. 0704-0188	
<p>The public reporting burden for this collection of information is estimated to average 1 hour per response, including the time for reviewing instructions, searching existing data sources, gathering and maintaining the data needed, and completing and reviewing the collection of information. Send comments regarding this burden estimate or any other aspect of this collection of information, including suggestions for reducing this burden, to Department of Defense, Washington Headquarters Services, Directorate for Information Operations and Reports (0704-0188), 1215 Jefferson Davis Highway, Suite 1204, Arlington, VA 22202-4302. Respondents should be aware that notwithstanding any other provision of law, no person shall be subject to any penalty for failing to comply with a collection of information if it does not display a currently valid OMB control number. <b>PLEASE DO NOT RETURN YOUR FORM TO THE ABOVE ADDRESS.</b></p>						
1. REPORT DATE (DD-MM-YY) July 2013		2. REPORT TYPE Final		3. DATES COVERED (From - To) 01 June 2010 – 31 May 2013		
4. TITLE AND SUBTITLE AQUEOUS SOLUTION HEAT PIPE TRANSPORT: QU-TUBE VS. CAPILLARY-PUMPED HEAT PIPE				5a. CONTRACT NUMBER In-house		
				5b. GRANT NUMBER		
				5c. PROGRAM ELEMENT NUMBER 62201F		
6. AUTHOR(S) Kenneth D. Kihm				5d. PROJECT NUMBER 2401		
				5e. TASK NUMBER		
				5f. WORK UNIT NUMBER Q03D		
7. PERFORMING ORGANIZATION NAME(S) AND ADDRESS(ES) The University of Tennessee Mechanical, Aerospace and Biomedical Engineering Dept. 414 Dougherty Engineering Bldg. Knoxville, TN 37996-2210				8. PERFORMING ORGANIZATION REPORT NUMBER AFRL-RQ-WP-TR-2013-0204		
9. SPONSORING/MONITORING AGENCY NAME(S) AND ADDRESS(ES) Air Force Research Laboratory Aerospace Systems Directorate Wright-Patterson Air Force Base, OH 45433-7542 Air Force Materiel Command United States Air Force				10. SPONSORING/MONITORING AGENCY ACRONYM(S) AFRL/RQHV		
				11. SPONSORING/MONITORING AGENCY REPORT NUMBER(S) AFRL-RQ-WP-TR-2013-0204		
12. DISTRIBUTION/AVAILABILITY STATEMENT Approved for public release; distribution unlimited.						
13. SUPPLEMENTARY NOTES PAO Case Number: 88ABW-2013-3488; Clearance Date: 07 Aug 2013. Report contains color. See also the related interim report, AFRL-RB-WP-TR-2012-0191 (DTIC ADA562203).						
14. ABSTRACT This report provides details on an in-house test effort that was conducted to evaluate the performance of a novel heat transfer device. The subject heat transfer device is one for which some intriguing performance claims have been made. Qu-tubes, or Advanced Thermal Transport Devices (ATTDs), are said to be entirely dry on the inside, act independently of gravity, exhibit very high conductivity, work over large distances and temperature ranges, and operate at a lower pressure than traditional heat pipes. The Aerospace Systems Directorate of the Air Force Research Laboratory purchased Qu-tubes and equipment to thoroughly examine the operation limits of such a device.						
15. SUBJECT TERMS Qu-tube, heat pipe, thermo-siphon, advanced thermal transport device, solid-state heat pipe						
16. SECURITY CLASSIFICATION OF:			17. LIMITATION OF ABSTRACT: SAR	18. NUMBER OF PAGES 62	19a. NAME OF RESPONSIBLE PERSON (Monitor) Andrew D. Swanson	
a. REPORT Unclassified	b. ABSTRACT Unclassified	c. THIS PAGE Unclassified			19b. TELEPHONE NUMBER (Include Area Code) N/A	

## TABLE OF CONTENTS

<b><u>Section</u></b>	<b><u>Page</u></b>
LIST OF FIGURES .....	ii
LIST OF TABLES .....	iv
1.0 SUMMARY .....	1
2.0 INTRODUCTION .....	2
3.0 QUALITATIVE CHARACTERIZATION USING IMAGING TECHNIQUES .....	4
3.1 Qu-tube (QT) and heat pipe (HP) samples .....	4
3.2 X-Ray Inspection of the Inside of the Cooled Samples.....	5
3.3 IR thermal Inspection: Qu-Tubes vs. Heat Pipes .....	7
3.4 Summary .....	17
4.0 QUANTITATIVE CHARACTERIZATION: QU-TUBES VS. HEAT PIPES.....	18
4.1 Experimental Set-Up Under a Controlled Environment.....	18
4.2 Experimental Test Matrices.....	22
4.3 Basic Performance Test: Qu-Tubes vs. Heat Pipes .....	25
4.4 Comparative Thermal Performance: Qu-Tubes vs. Heat Pipes.....	29
4.5 Effective Thermal Conductivities: Qu-Tubes vs. Heat Pipes .....	40
5.0 CONCLUSIONS AND RECOMMENDATIONS .....	50
6.0 REFERENCES .....	52

# LIST OF FIGURES

<b><u>Figure</u></b>	<b><u>Page</u></b>
Figure 1: Schematic Configuration of the Two Tested Heat Pipes (HP-1 and HP-2) and the Two Tested Qu-Tubes (QT-1 and QT-2).....	5
Figure 2: X-Ray Images of Copper-Water Heat Pipes.....	6
Figure 3: X-Ray Images of Aluminum Qu-Tubes .....	7
Figure 4: Example Imaging Configurations.....	9
Figure 5: Progressive IR Images for the V-Meniscus of HP-1(left) and HP-1-N (right).....	10
Figure 6: Progressive IR Images for the V-Meniscus of QT-1 (left) and HP-1 (right).....	11
Figure 7: Progressive IR Images for the H-Meniscus of QT-1 (left) and HP-1 (right).....	13
Figure 8: Progressive IR Images for the NH-Meniscus of QT-1 (left) and HP-1 (right).....	14
Figure 9: Progressive IR Images for the NH-Meniscus of QT-1 (left) and HP-1-N (right).....	14
Figure 10: Progressive IR Images for the V-Meniscus of QT-1 (left) and HP-1-N (right) .....	15
Figure 11: Progressive IR Images for the H-Meniscus of QT-1 (left) and HP-1-N (right) .....	16
Figure 12: Experimental Set-Up: (a) the Adjustable Inclination of the Test Article, (b) the Schematic of the Experimental Set-Up, and (c) the Cincinnati Sub-Zero (CSZ) Chamber.....	20
Figure 13: (a) Front-End Interface of the LabView VI Data Acquisition Program, and (b) Typical Readout Screens for the Thermocouple Temperature Data.....	21
Figure 14: Axial Temperature Distributions for the Adiabatic Regions.....	26
Figure 15: Basic Performance Data for the 5/8 in. Qu-Tube (QT-2).....	27
Figure 16: Basic Performance Data for the 5/8 in. Heat Pipe (HP-2).....	28
Figure 17: Time History of Temperature Distributions and Heat Input/Output at Inclination Angle of +5 deg. (Condenser Upward) and Coolant Temperature of 40°C .....	32
Figure 18: Time History of Temperature Distributions and Heat Input/Output at Inclination Angle of +5 Degrees (Condenser Upward) and Coolant Temperature of 20°C.....	33
Figure 19: Time History of Temperature Distributions and Heat Input/Output at Inclination Angle of +5 Degrees (Condenser Upward) and Coolant Temperature of 60°C.....	34
Figure 20: Time History of Temperature Distributions and Heat Input/Output at Inclination Angle of +1 Degree (Condenser Upward) and Coolant Temperature of 40°C .....	35
Figure 21: Time History of Temperature Distributions and Heat Input/Output at Inclination Angle of +5 Degrees (Condenser Upward) and Coolant Temperature of 40°C.....	36
Figure 22: Time History of Temperature Distributions and Heat Input/Output at Inclination Angle of +5 Degrees (Condenser Upward) and Coolant Temperature of 20°C.....	37
Figure 23: Time History of Temperature Distributions and Heat Input/Output at Inclination Angle of +5 Degrees (Condenser Upward) and Coolant Temperature of 60°C.....	38
Figure 24: Time History of Temperature Distributions and Heat Input/Output at Inclination Angle of +1 Degree (Condenser Upward) and Coolant Temperature of 40°C .....	39
Figure 25: Effective Thermal Conductivity at Inclination Angle of +5 Degrees (Condenser Upward) and Coolant Temperature of 40°C.....	42
Figure 26: Effective Thermal Conductivity at Inclination Angle of +5 Degrees (Condenser Upward) and Coolant Temperature of 20°C.....	43

Figure 27: Effective Thermal Conductivity at Inclination Angle of +5 Degrees (Condenser Upward) and Coolant Temperature of 60°C.....	44
Figure 28: Effective Thermal Conductivity at Inclination Angle of +1 Degree (Condenser Upward) and Coolant Temperature of 40°C.....	45
Figure 29: Effective Thermal Conductivity at Inclination Angle of +5 Degrees (Condenser Upward) and Coolant Temperature of 40°C.....	46
Figure 30: Effective Thermal Conductivity at Inclination Angle of +5 Degrees (Condenser Upward) and Coolant Temperature of 20°C.....	47
Figure 31: Effective Thermal Conductivity at Inclination Angle of +5 Degrees (Condenser Upward) and Coolant Temperature of 60°C.....	48
Figure 32: Effective Thermal Conductivity at Inclination Angle of +1 Degree (Condenser Upward) and Coolant Temperature of 40°C.....	49

## LIST OF TABLES

<b><u>Table</u></b>	<b><u>Page</u></b>
Table 1: List of the Inventor's Patents for Qu-Tubes .....	3
Table 2: Experimental Matrix for Infra-Red Imaging.....	8
Table 3: Heater Insert Material Properties .....	19
Table 4: Test Matrix for the 36 in. (L) x 0.5 in. (D) Wicked Copper Heat Pipe (HP-1) .....	23
Table 5: Test Matrix for the 36 in. (L) x 0.5 in. (D) Aluminum Qu-Tube (QT-1) .....	23
Table 6: Test Matrix for the 36 in. (L) x 5/8 in. (D) Wicked Copper Heat Pipe (HP-2) .....	24
Table 7: Test Matrix for the 36 in. (L) x 5/8 in. (D) Aluminum Qu-Tube (QT-2) .....	24
Table 8: Test Parameters for Figures 17 to 24 .....	30
Table 9: Test Parameters for Figures 25 to 32 .....	41

## 1.0 SUMMARY

Dr. Yuzhi Qu's 1991 patent (CN 1,048,593) seemed to have intrigued the heat pipe cooling research and development area with the invention of the solid state heat pipe (SSHP), known also as "super tubes" or "Qu-tubes." These purportedly superior tubes were claimed to have such desirable qualities as entirely dry operation, gravity-independence, super conductivity, and compatibility with various tube materials over broad ranges of distance, temperature, and time. These qualities would indeed revolutionize the entire field of two-phase heat pipe cooling, with practical applications in designing thermal management systems for future high-speed vehicles. Despite a number of investigative efforts by nationally leading research teams including NASA LaRC [1], University of Alabama [2], UCLA [3] and AFRL [4], no conclusive evidence has yet been reached confirming the inventor's claims regarding these Qu-tubes.

The present research aimed to test these inventor's claims by comparing the thermal performance of two 36"-long aluminum Qu-tubes of 1/2 in. and 5/8 in. in diameter, respectively (Posnett Corp.), with two copper heat pipes of corresponding dimensions (Thermacore Inc.) through several individual experiments. The "Qu-tubes" used in this investigation were not certified by the inventor but manufactured to match the original design as determined through testing. These experimental investigations used such tools as X-ray and infrared (IR) imaging for qualitative/semi-quantitative characterization and, more substantially, used an environmentally controlled thermal test stand with a comprehensive LabView DAQ system for more detailed and quantitative characterization by varying such parameters as tube type, diameter, coolant temperature, evaporator/condenser tilt angle, and heater power input.

The devices investigated in this effort were obtained from the Posnett Corporation, a U.S. manufacturer of Inorganic Aqueous Solution (IAS) heat pipes. IAS has been identified as the critical working material in Qu-tube devices [3] that gives them the extraordinary performance characteristics. The results of our experiments did not support the claims regarding the Qu-tubes. According to the test results, the Qu-tubes may not be entirely dry during operation; they are in fact less stable, efficient, and conductive than conventional heat pipes of corresponding sizes; and the Qu-tubes are most likely gravity-dependent. Our detailed and quantitative findings suggest that the devices we purchased are not revolutionary in performance, and may in fact perform worse than the capillary-pumped heat pipes in several key functions. The lack of physical resources and scarcity of valid scientific information about Qu-tubes has deterred considering a more extensive and comprehensive investigation.

## 2.0 INTRODUCTION

The focus of this test effort is on a heat transfer device known under a variety of names, but which is most often called a Qu-tube after its inventor, Dr. Yuzhi Qu (Table 1). It is also referred to as a solid state heat pipe (SSHP) or a “super tube”. This device was advertised as utilizing a new heat transfer principle and as being superior to standard heat pipes, which certainly intrigued both the academic and the governmental research laboratories associated with the two-phase heat pipe cooling community.

The device, from outer appearances, looks like a heat pipe, which is a sealed tube with an interior wick and working fluid that absorbs and rejects energy through liquid/vapor phase change in a passive manner. The Qu-tube, or SSHP, was claimed to be entirely dry on the inside and to consist of three thin layers of material and a powder. A number of claims have been made by the inventor. The creator reports that these are solid state devices, act independently of gravity, exhibit super conductivity (up to 14 MW/m·K), have a high heat transfer density – theoretically 27.2MW/m<sup>2</sup> in axial and 158kW/m<sup>2</sup> in the radial direction, work over large distances and large temperature ranges (-65 ~ 1,100°C), have long operation hours (110,000 hours) and operate at a lower pressure than do traditional heat pipes. Additional claims include good compatibility with tube materials without generating non-condensable gases and radiation safety for Beta ray and neutron emission.

Unfortunately, none of the listed patents in Table 1 provides any formidable physical evidence or convincing explanations on how the claimed Qu-tube works scientifically. For example, one of the patents, US 6,132,823, claimed a measured effective thermal conductivity of 3,183,000 W/m·K, which is one to two orders-of-magnitude larger than the current state-of-the-art heat pipe conductivities, which range from 50,000 to 200,000 W/m·K. Furthermore, the claim of solid-state operation has not been fully interrogated to examine whether the Qu-tube actually defies the influence of gravity. Some results presented in this report indicate the presence of liquid and gravity-dependence.

**Table 1: List of the Inventor's Patents for Qu-Tubes**

File Numbers	Published Dates
CN 1,048,593 (Chinese patent)	January 16, 1991
WO 98/19859 (Intl. application publication)	May 14, 1998
US 6,132,823	October 17, 2000
US 6,811,720 B2	November 2, 2004
US 2005/0056807 A1 (patent application publication)	March 17, 2005
US 6,916,430 B1	July 12, 2005

In summary, the inventor's statements do not seem like 'expert' language and are very broad. Additionally, early tests by others, such as NASA LaRC [1], University of Alabama [2], UCLA [3] and AFRL [4] did not always substantiate the claims, outright refuted some of the claims, revealed various operational anomalies, were often inconclusive, and had contradictory results. The most recent publication from the Propulsion Directorate of AFRL [4] presented a statement about the inventor's claims as follows: "In conclusion, this investigation did not find anything substantive in these devices to validate any new phenomenon or breakthrough in heat transport capacity that exceeded what the state of the art heat pipe technology can offer. However, the authors would like to emphasize again that the tested tubes were not certified by either the inventor or the manufacturer as "super tubes".

This reveals a lack of understanding of the physics involved and the necessity of a scientifically-driven research program. The USAF thus initiated a research effort to add the scientific rigor required to determine the underlying physics by devising systematic examinations of the Qu-tubes under thermally controlled environments and establish a very extensive database of Qu-tube operations. In order to examine the primary claim of the Qu-tube's dramatically superior performance, all of the Qu-tube data should be comprehensively compared with corresponding heat pipe data under identical operation conditions. Henceforth, the main goal of this report is to investigate the "super conductivity" claim of the Qu-tube in rigorous comparisons with capillary-pumped heat pipes. Imaging and thermal test results also support solid-state and gravity-dependence conclusions.

Section 2 of this report presents qualitative visual characterizations and comparisons of the Qu-Tube and heat pipe operations, through X-ray imagery and IR thermography. Section 3 presents quantitative thermal characterizations and comparisons of the Qu-Tube and heat pipe operations in a controlled environment. Finally, Section 4 presents concluding remarks.

### **3.0 QUALITATIVE CHARACTERIZATION USING IMAGING TECHNIQUES**

This chapter presents qualitative visual characterizations of the Qu-Tube and heat pipe by using both X-ray imagery and IR thermography. The main objective for this visual inspection is three-fold: (1) to examine the inside of Qu-tubes via X-ray, (2) to map the surface temperature variations via IR imaging, and (3) to compare these findings with conventional wicked and non-wicked heat pipes under identical heating conditions. Section 3.1 describes the test articles, two Qu-tubes and two heat pipes, and Section 3.2 presents the X-ray images of the test articles. Section 3.3 presents the IR thermographic images of the test articles under heating.

#### **3.1 Qu-tube (QT) and heat pipe (HP) samples**

Figure 1 shows the test samples of two copper wicked heat pipes of 1/2-inch (HP-1) and 5/8-inch (HP-2) diameter, which were manufactured by Thermacore Inc., and two aluminum Qu Tubes of 1/2-inch (QT-1) and 5/8-inch (QT-2) diameter, which were manufactured by Posnett Corp. All of the samples are 36-inches in length.

The evaporator ends of the Qu-tubes are capped with aluminum plugs and welded to the aluminum cylinder body. Under high-temperature operation, this welded joint, which is inserted into a stainless steel heater shoe (refer to Fig 12), is subjected to extremely high thermal and structural stresses and can become breached. This substantially limits the maximum test temperature of the Qu-tubes in order to reduce the risk of cracks and leaks of the internal materials. While this welded tube design may limit the maximum temperature achieved in testing, the most critical performance characteristics could still be evaluated. The rounded evaporator end of the heat pipe is forged to form a single piece with the cylindrical section. The condenser ends of all of the tested samples are pinch-sealed.



- (a) **HP-1:** copper-water heat pipe with sintered wicking;  $L = 36''$  and  $D = 1/2''$ . The rounded end (the left end) is forged and the fill-tube is pinch-sealed (the right end).



- (b) **HP-2:** copper-water heat pipe with sintered wicking;  $L = 36''$  and  $D = 5/8''$ . The rounded end is forged and the fill-tube is pinch-sealed.



- (c) **QT-1:** aluminum Qu-tube with no wicking;  $L = 36''$  and  $D = 1/2''$ . The flat end-cap is welded (the left end) and the fill-tube is pinch-sealed (the right end).



- (d) **QT-2:** aluminum Qu-tube with no wicking;  $L = 36''$  and  $D = 5/8''$ . The flat end-cap is welded and the fill-tube is pinch-sealed.

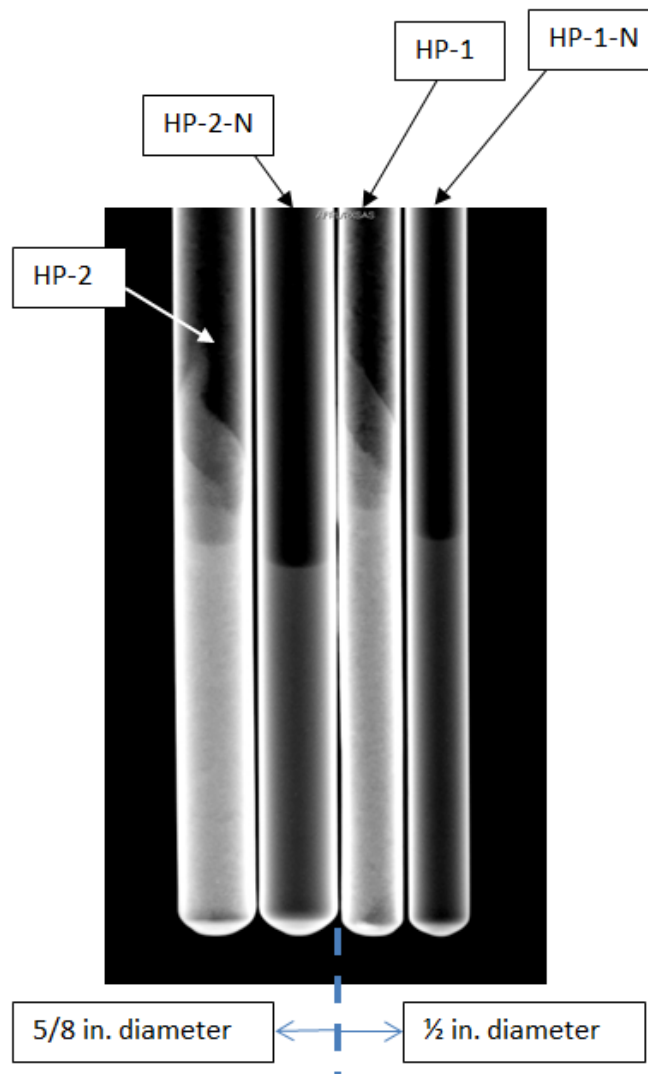
**Figure 1: Schematic Configuration of the Two Tested Heat Pipes (HP-1 and HP-2) and the Two Tested Qu-Tubes (QT-1 and QT-2)**

### 3.2 X-Ray Inspection of the Inside of the Cooled Samples

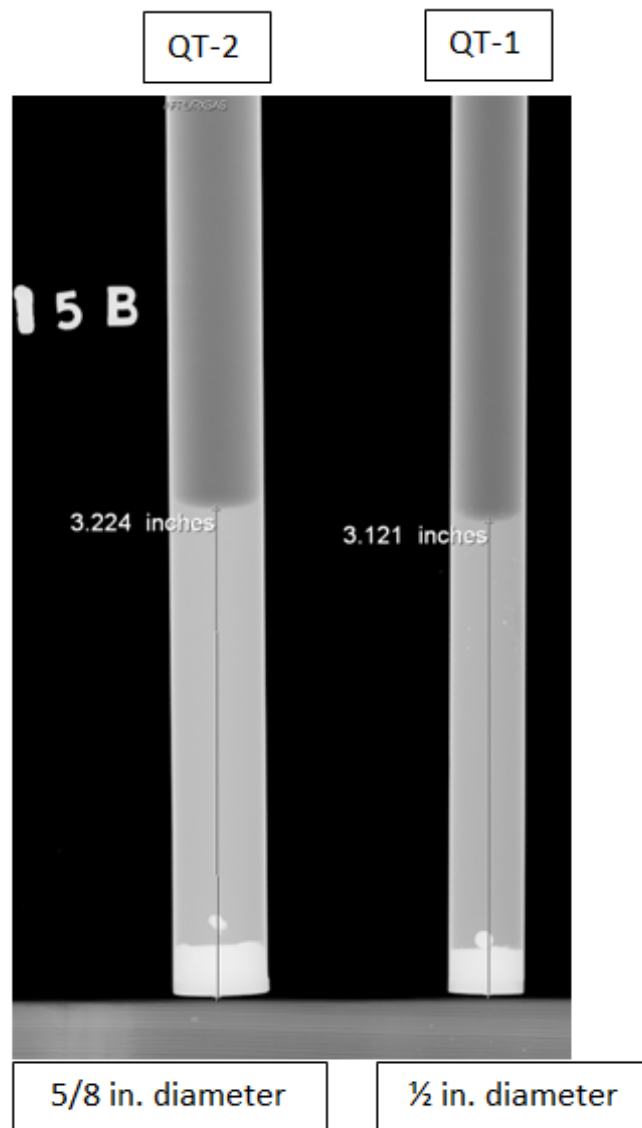
The high-resolution X-ray imaging facility at the Air Force Research Laboratory (AFRL) Materials & Manufacturing Directorate at Wright-Patterson Air Force Base allowed examination of the inside of the test samples and could verify the existence of working fluid or coolant materials inside the Qu-tubes.

Figure 2 shows the water coolant contained inside the wicked (HP-1 and HP-2) heat pipes and non-wicked (HP-1-N and HP-2-N) heat pipes. The wicking layers are more densely laid near the meniscus areas. The heights of the menisci range from 3.5'' to 4.0'', as measured from the bottom end. All of the evaporator ends show no welding joints.

Figure 3 clearly identifies the existence of a working fluid or substance for the tested Qu-tubes, despite the inventor's claim that the Qu-tubes are entirely dry on the inside. The X-ray images, however, are unable to indicate whether this working fluid is in the form of pure liquid, slurries, or fine powders. It is also apparent that the working fluid substance is gravitationally settled to the evaporator section of the cold Qu-tubes. Thus, the Qu-tube operations can significantly depend on gravity. The heights of the menisci, or the interfaces of unknown coolant material, range from 3.1 in. to 3.2 in., as measured from the bottom end. Additionally, the end plugs at the evaporator bottom ends are clearly visible, showing the weld discontinuities.



**Figure 2: X-Ray Images of Copper-Water Heat Pipes**



**Figure 3: X-Ray Images of Aluminum Qu-Tubes**

### 3.3 IR thermal Inspection: Qu-Tubes vs. Heat Pipes

In order to achieve a qualitative understanding of the thermal operations of the test samples, a total of twenty (20) infrared (IR) thermal imaging video files were recorded for both 1/2" Qu-tubes (QT-1) and 1/2" heat pipes (HP-1 & HP-1-N) during heating with a heat gun.

The detailed test conditions for these IR recordings are summarized in Table 2. Note that "N" represents non-wicking. For example, HP-1-N represents the 1/2 in.-diameter heat pipe with no wicking inside. The letters "V", "H" and "NH" denote the tube inclinations as vertical, positive horizontal (+5° inclination), and negative horizontal (-5° inclination) orientations, respectively.

Also, “-meniscus” stands for heating near the meniscus, while “-bottom” stands for heating near the evaporator’s bottom end.

The heating was provided by a heat gun, which expelled hot air to either the bottom of the evaporator (“Evaporator bottom” – Fig 4 (a)) or to the approximate meniscus area (“Meniscus area” – Fig 4 (b)). Figure 4 (b) shows that the HP-1 and the QT-1 samples are aligned to match their menisci locations with the center of the heat gun outlet. Note that the menisci heights of the heat pipe samples are taller than those of the Qu-tube samples by approximately 0.4 in. to 0.8 in. (refer to Section 2-2).

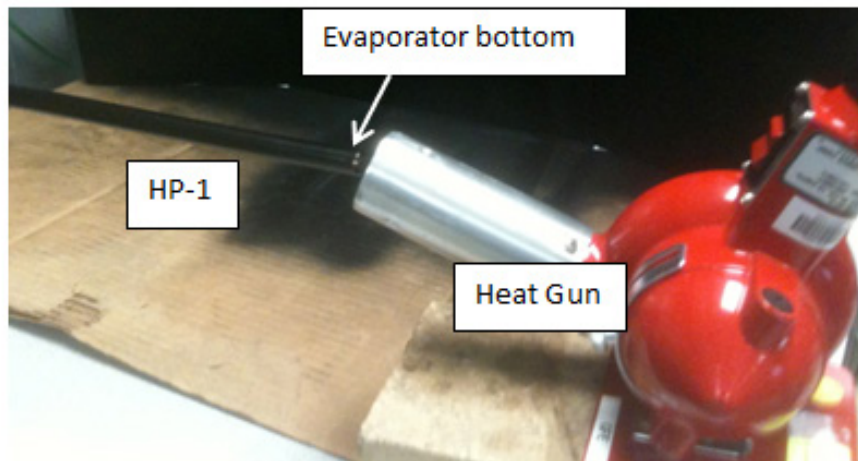
The diagonal components in Table 2 correspond to the single-tube IR images, for QT-1, HP-1 or HP-1-N. All of the IR images were recorded at a rate of 20 frames-per-second (fps). The off-diagonal components correspond to the IR images for both QT-1 and HP-1, side-by-side. This report presents only those comparative IR images corresponding to the off-diagonal component conditions, as marked in red in Table 2. Also, only the cases of meniscus heating are presented, since the cases of bottom heating are not directly relevant to ordinary operations of the test samples.

**Table 2: Experimental Matrix for Infra-Red Imaging**

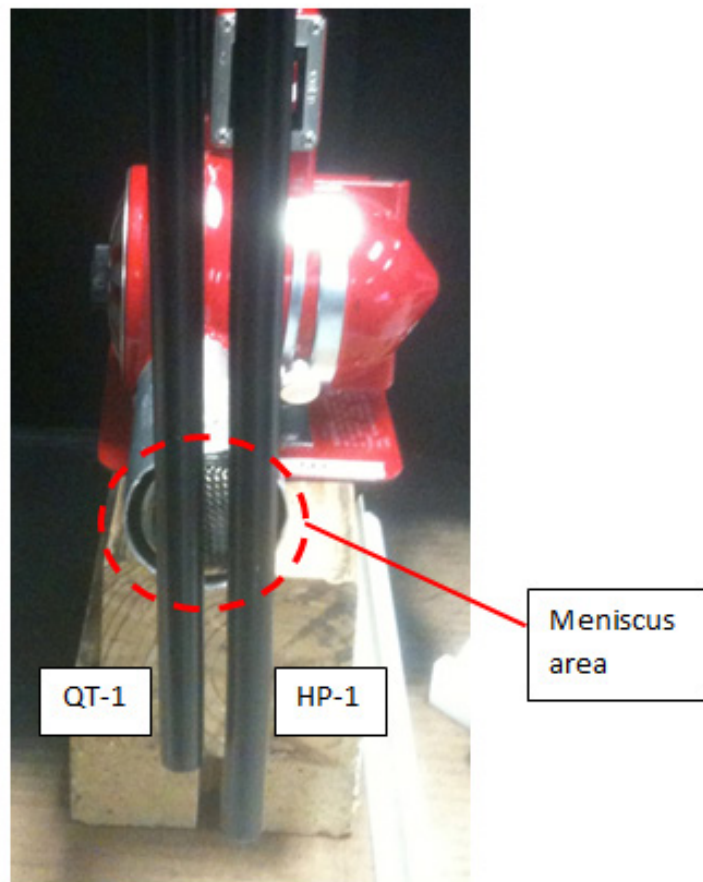
Test	QT-1 (L = 36 in., D = ½ in.)	HP-1 (wicked) (L = 36 in., D = ½ in.)	HP-1-N (non-wicked) (L = 36 in., D = ½ in.)
QT-1	V-bottom V-meniscus H-bottom H-meniscus		
HP-1	V-bottom V-meniscus (Fig. 6) H-meniscus (Fig. 7) NH-meniscus (Fig. 8)	V-bottom V-meniscus H-bottom H-meniscus	
HP-1-N	V-bottom V-meniscus (Fig. 10) H-meniscus (Fig. 11) NH-meniscus (Fig. 9)	V-meniscus (Fig. 5)	V-bottom V-meniscus

Legend:

V: Vertical orientation  
H: Positive horizontal orientation (+5°)  
NH: Negative horizontal orientation (-5°)  
-bottom: The heat gun was aimed at the evaporator end.  
-meniscus: The heat gun was aimed at the meniscus area.



(a) Single-tube imaging condition of "H-bottom"



(b) Comparative imaging condition of "V-meniscus"

**Figure 4: Example Imaging Configurations**

Figure 5 shows progressive and comparative IR images for HP-1 (left) and HP-1-N (right) in their vertical orientations, heated near the menisci areas.

For the case of heat pipe with no wicking (HP-1-N), the return of condensed coolant is driven only by gravity, and the insufficient amount of return makes the evaporator dry out, with meniscus fluctuations occurring as early as  $t = 60$  s. As a result, the surface temperature profiles oscillate, and their distributions along the tube are highly nonuniform.

For the case of wicked heat pipe (HP-1), a sufficient amount of condensed coolant returns, driven by the wicking capillary force as well as by gravity. A steady two-phase passive heat transfer mode is established, allowing the uniform temperature profile development along the entire tube length. Furthermore, the surface temperature of HP-1 is substantially lower than that of HP-1-N.

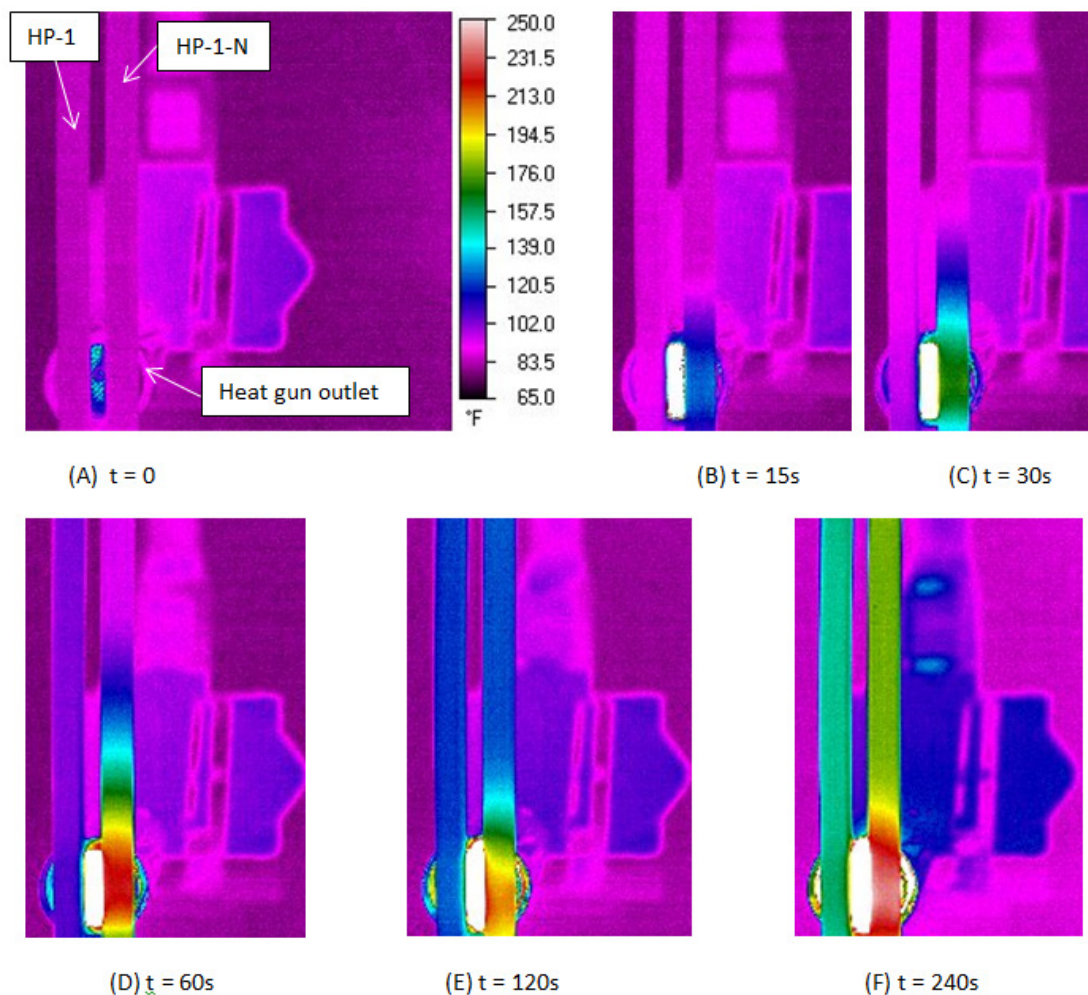


**Figure 5: Progressive IR Images for the V-Meniscus of HP-1(left) and HP-1-N (right)**

Figure 6 shows progressive and comparative IR images for QT-1 (left) and HP-1 (right) in their vertical orientations, which were heated near the menisci areas.

Oscillating temperature profiles are triggered in the Qu tube (QT-1) near the meniscus region during the period from  $t = 190\text{s}$  to  $192\text{s}$ ; then, the fluctuation mode repeats irregularly. This is believed to be caused by the evaporator dry-out because of an insufficient amount of condensed coolant return in the Qu-tube without wicking, which is very similar to the previous case of the heat pipe without wicking (HP-1-N). Furthermore, the observed fluctuations of the temperature profiles suggest- that the Qu-tube contains some type of working fluid and is not gravity-independent.

The wicked heat pipe (HP-1) establishes a steady two-phase passive heat transfer mode, allowing for a gradual and uniform temperature profile development along the tube.

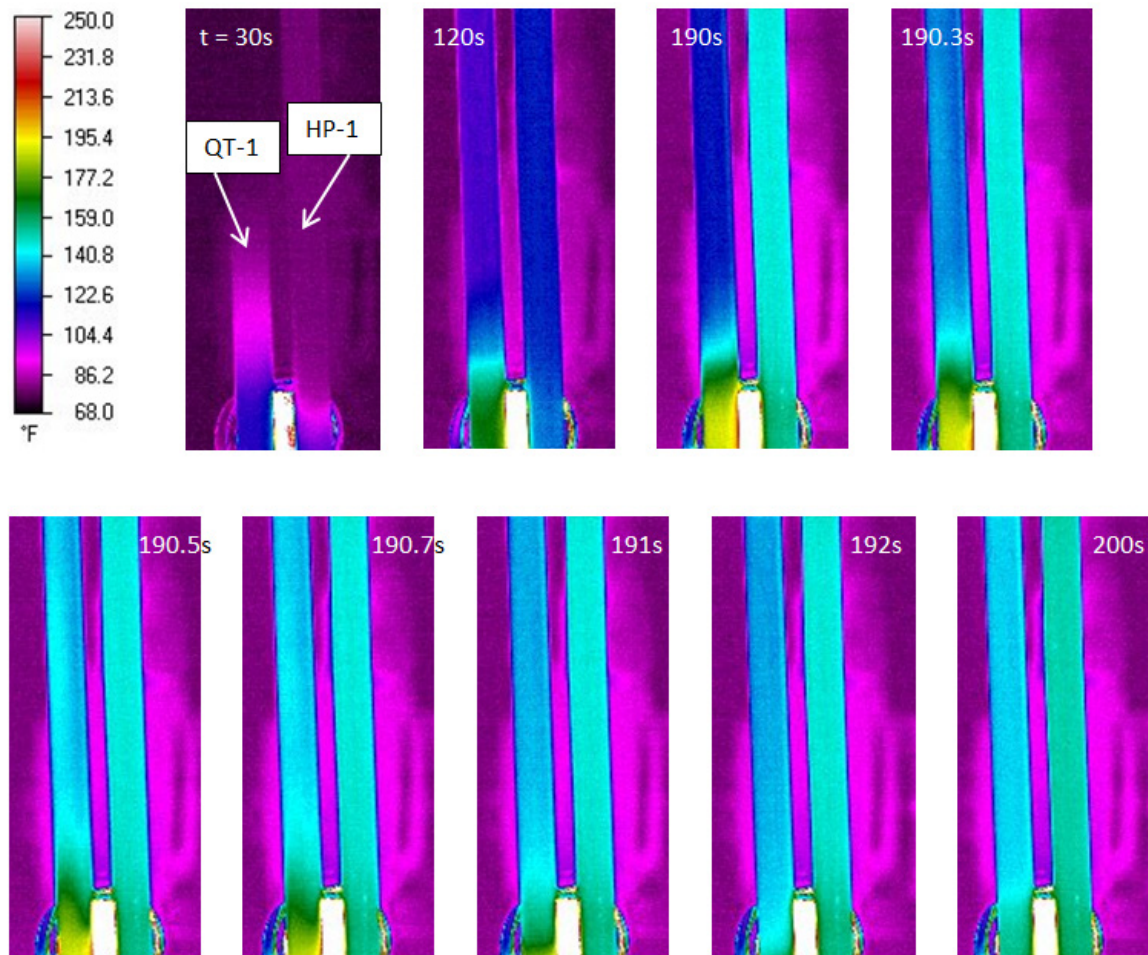
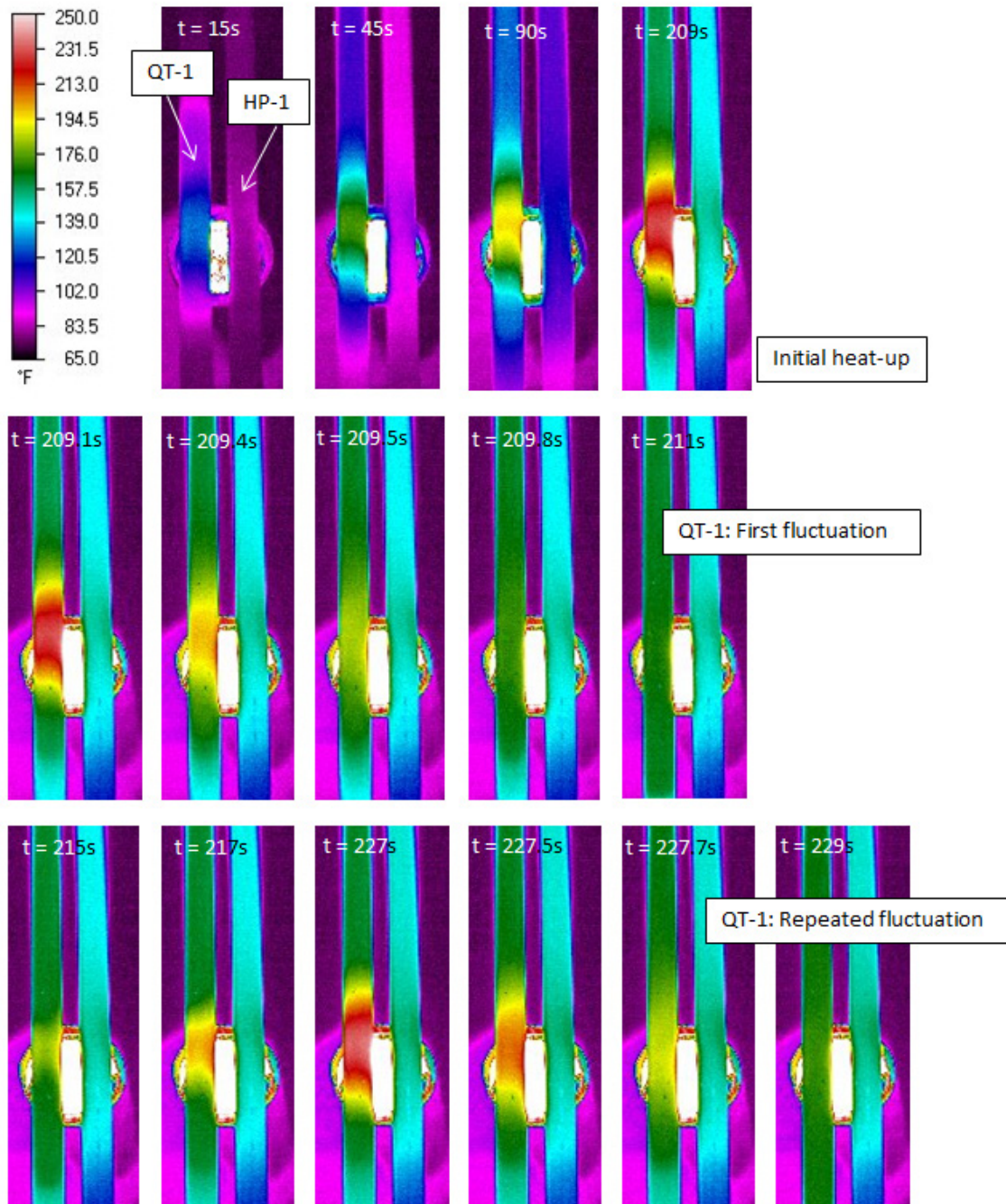


**Figure 6: Progressive IR Images for the V-Meniscus of QT-1 (left) and HP-1 (right)**

Figure 7 shows progressive and comparative IR images for QT-1 (left) and HP-1 (right) in their near horizontal orientation ( $+5^\circ$  inclination), which were heated near their menisci areas.

During the initial heating period, up to  $t = 209$  sec (the first row of images), the temperature near the meniscus area of the Qu-tube (QT-1) rises very rapidly, while the wicked heat pipe (HP-1) develops more uniform temperature along the entire tube. Similar to the previous vertical heating case (Fig. 6), it is believed that this distinction is caused by the fact that the Qu-tube has no wick inside. For the tube surface area above the meniscus, the aluminum Qu-tube reaches higher temperatures and seemingly steeper temperature gradients, in comparison with those of the copper heat pipe. This implies that the effective thermal conductivity of the Qu-tube may be lower than that of the heat pipe, if we assume an identical cooling heat transfer rate, which is equivalent to the effective thermal conductivity multiplied by the temperature gradient. Similar observations prevail as time progresses, showing steeper temperature gradients and a higher maximum temperature for QT-1 and more uniform and gradual temperature profiles for HP-1.

When the temperature non-uniformity of QT-1 exceeds a certain limit at  $t = 209$ s, the first sudden surge of the working fluid is triggered, and the inside is seemingly flooded with the fluid, which momentarily results in the uniform temperature distributions (the second row of images). This jolting continues repeatedly, but with progressively shorter intervals and reduced strengths. In contrast, the heat pipe raises the surface temperature gradually and uniformly, ensuring a significantly more stable operation. The surface temperature of QT-1 is also significantly higher than that of HP-1 for the present horizontal heating case, whereas the difference was insignificant for the vertical heating case, as previously shown in Figure 6.



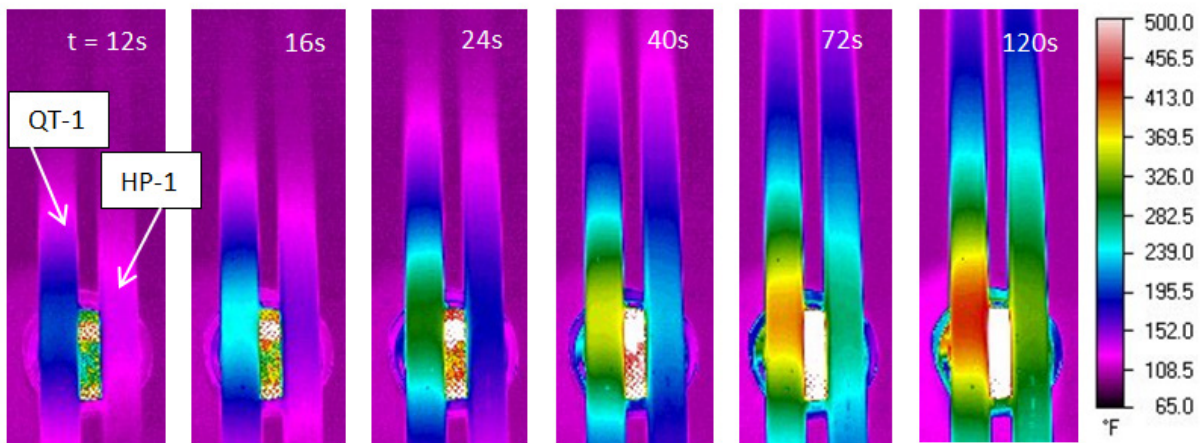
**Figure 7: Progressive IR Images for the H-Meniscus of QT-1 (left) and HP-1 (right)**

Figure 8 shows progressive and comparative IR images for QT-1 (left) and HP-1 (right) in their negative horizontal orientations ( $-5^\circ$  inclination), which were heated near their menisci areas.

For both QT-1 and HP-1 at  $-5^\circ$  inclination from horizon, their evaporator sections are located higher than their condenser sections. Thus, the internal working fluids flow toward the condenser

sections by gravity and their evaporator sections contain no working fluids and no menisci. The heating of the menisci areas (the menisci locations when the tubes are vertically oriented) is unable to initiate a two-phase heat transfer mode. Instead, the surface temperature reflects the heat conduction of the tube materials. The relatively lower conductivity of the aluminum shell of QT-1, in comparison to that of the copper shell of HP-1, results in steeper temperature gradients along the tube and a higher maximum temperature occurring near the heated spot. Thus, the inventor's claim of gravity independence is not supported for the tested Qu-tube sample.

Figure 9 shows IR images for QT-1 and HP-1-N in the same configuration as in Figure 8. Similar observations resulted: whether the heat pipe has wicking (HP-1) or not (HP-1-N), the heat conduction of the tube materials determined the development of the surface temperature profiles.



**Figure 8: Progressive IR Images for the NH-Meniscus of QT-1 (left) and HP-1 (right)**

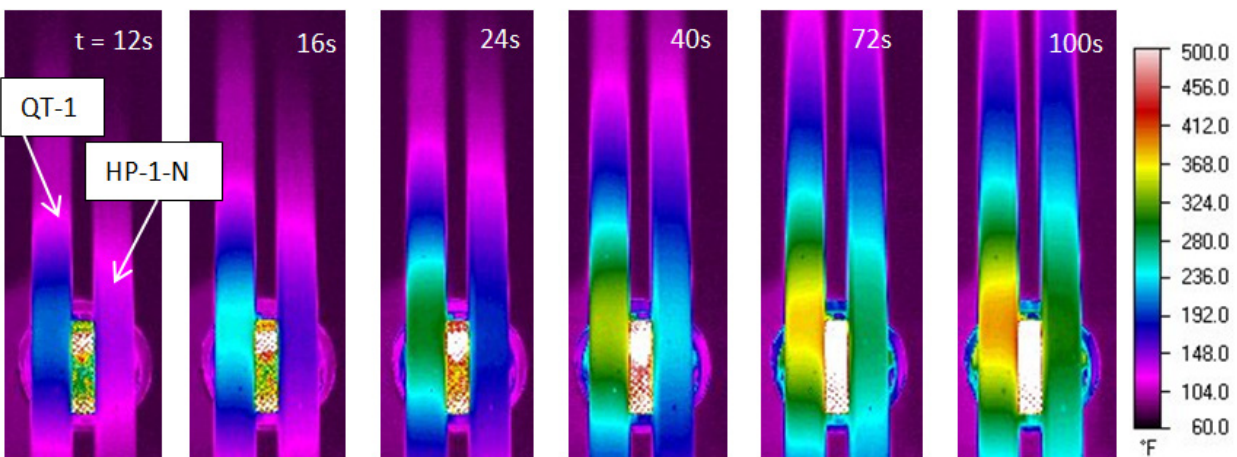


**Figure 9: Progressive IR Images for the NH-Meniscus of QT-1 (left) and HP-1-N (right)**

Figure 10 shows progressive and comparative IR images for QT-1 (left) and HP-1-N (right) in their vertical orientations, which were heated near the menisci areas.

For the heat pipe with no wicking (HP-1-N), as previously shown in Figure 5, the condensed coolant returns were insufficient to prevent the dry-out of the evaporator. The first fluctuations were observed during the period from  $t = 146\text{s}$  to  $148\text{s}$ ; thereafter, weaker fluctuations repeatedly occurred. As a result, the surface temperature profiles oscillated, and they were highly nonuniform.

The Qu-tube (QT-1) triggered the fluctuations at a later time: at approximately  $t = 200\text{s}$ , and the fluctuation repeated thereafter, as similarly shown in Figure 6. This is also believed to be attributed to the evaporator dry-out because of insufficient condensed coolant return in the Qu-tube with no wicking, which indeed is very similar to the case of heat pipe with no wicking (HP-1-N). The maximum temperature of QT-1 occurring near the heated meniscus area is significantly lower than that of HP-1-N, whereas it is substantially higher than that of HP-1.

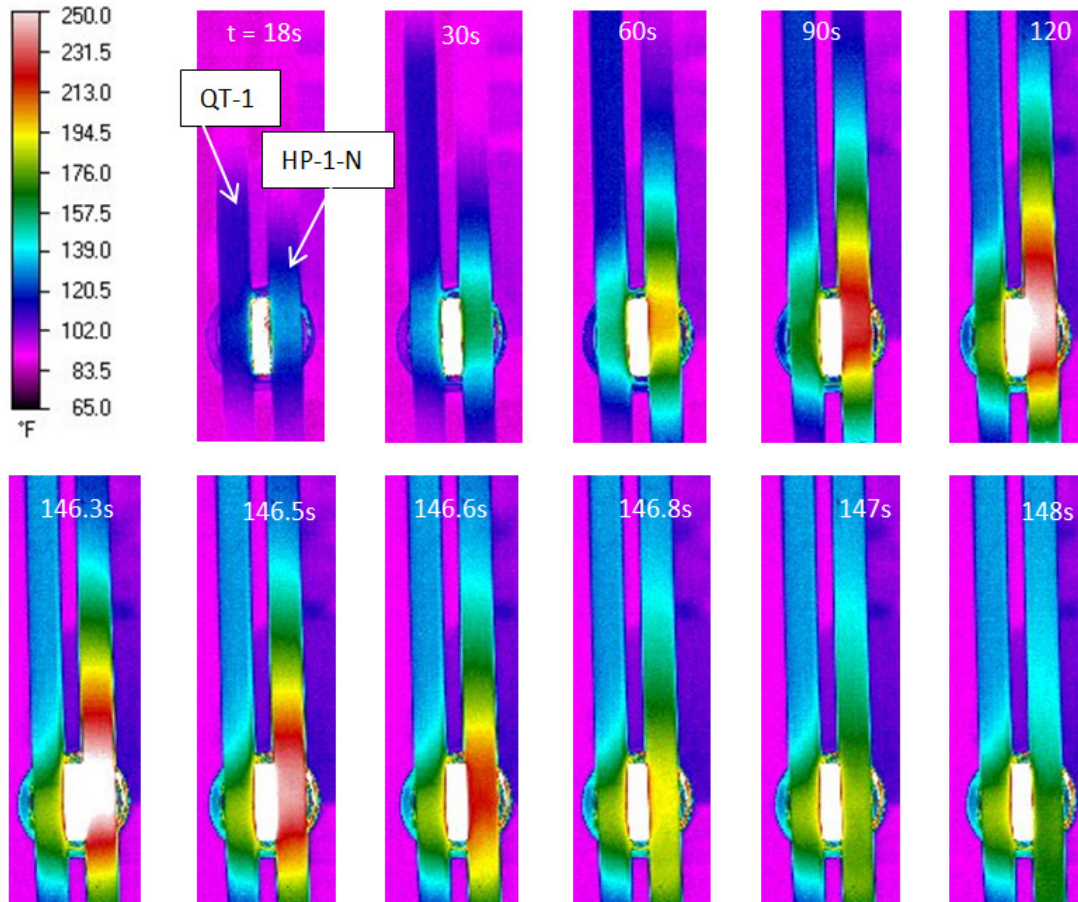


**Figure 10: Progressive IR Images for the V-Meniscus of QT-1 (left) and HP-1-N (right)**

Figure 11 shows progressive and comparative IR images for QT-1 (left) and HP-1-N (right) in their positive horizontal orientations ( $+5^\circ$  inclination), which were heated near the menisci areas.

Both QT-1 and HP-1-N show repeated fluctuations driven by the dry-out of their evaporator sections, which resulted from insufficient coolant returns in the absence of the capillary action due to no wicking inside the tubes. The strength of the fluctuations seems to be relatively weaker for the present horizontal orientations than in the cases of the vertical orientations, since the corresponding level of the dry-out should be less severe for the former case. The maximum temperature near the meniscus area of HP-1-N is higher than that of QT-1, which is similar to the vertically heated case (Figure 10).

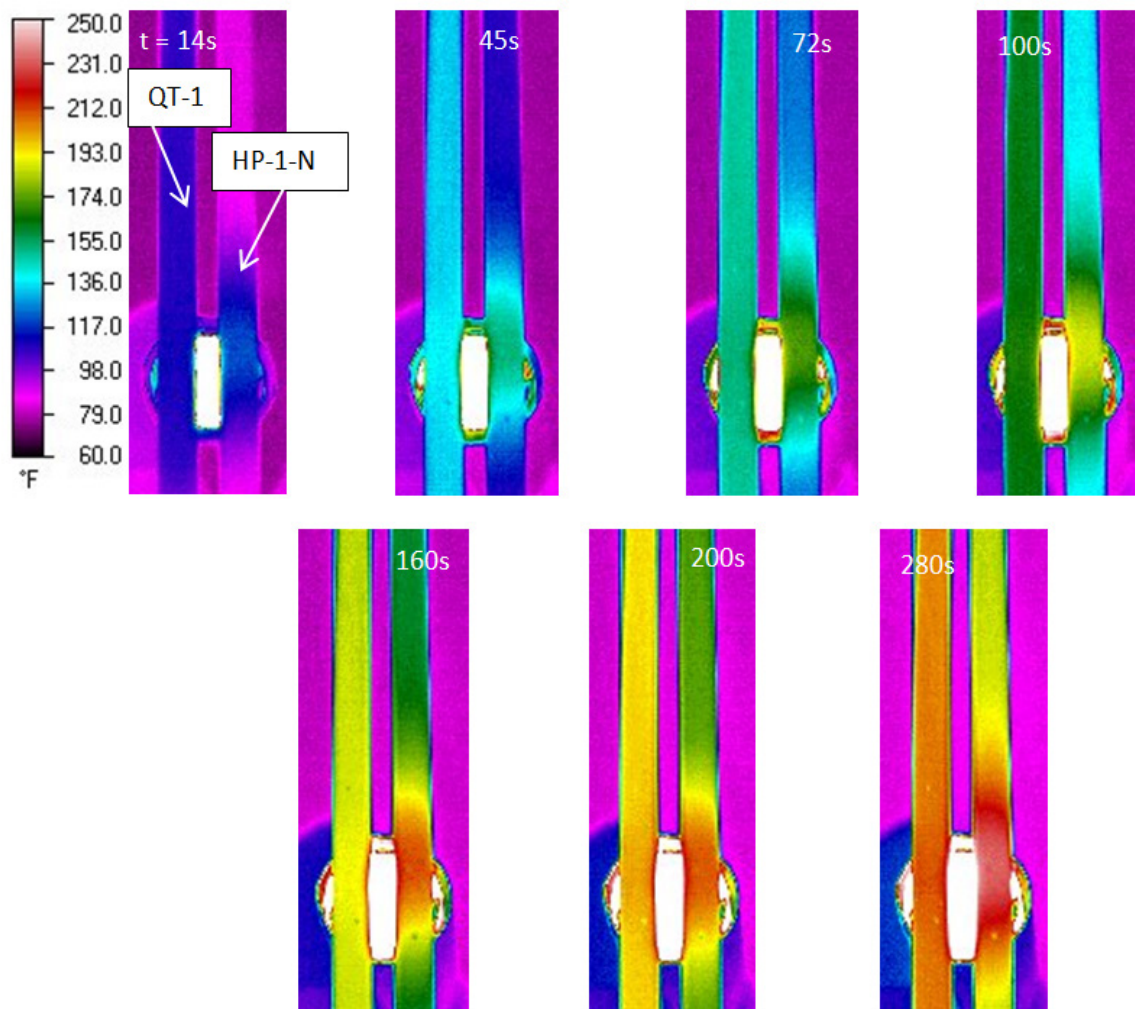


**Figure 11: Progressive IR Images for the H-Meniscus of QT-1 (left) and HP-1-N (right)**

### 3.4 Summary

The X-ray imaging of the inside of the Qu-tubes reveals “meniscus-like” interfaces for both QT-1 and QT-2, which seems to show the existence of an unknown working fluid. However, such an interface could also have resulted with extremely fine powder materials, instead of fluid. Thus, at present, this finding is inconclusive, and a dynamic X-ray imaging while the tubes are being tilted, and/or chemical analysis of the inside materials, could provide more solid evidence.

Based on comparative observations of all of the recorded IR image files, the Qu-tube responds more rapidly to heat input during start-up, while the wicked heat pipe (HP-1) provides slower starts but a more stable operation. Almost always, QT-1 is subjected to periodically repeating fluctuations of the surface temperature profiles, as well as to jolting movements of the internal unknown materials (fluid or fine powder). Note that the non-wicked heat pipe (HP-1-N) shows the most unstable operation among the three tested samples.

The Qu-tube shows a higher maximum temperature near the menisci, in comparison with the wicked heat pipe. However, it shows a somewhat lower maximum temperature than the non-wicked heat pipe (HP-1-N). The relatively larger temperature gradients along the Qu-tube suggest its relatively lower effective thermal conductivities, compared to those of the wicked heat pipe. Thus, the Qu-tube appears to be somewhat less effective in the overall two-phase heat transfer than the wicked water heat pipe.

However, considering that the present experimental conditions, such as heating and cooling, were not rigorously controlled, these observations are prone to qualitative judgments. Therefore, a more concrete conclusion is postponed until a quantitative examination under a controlled environment can be completed. Indeed, the next chapter presents more detailed quantitative measurement data for heat flux and temperature profiles under a controlled environment, which provide more solid evidence for most of the observations and preliminary conclusions obtained from the aforementioned qualitative examinations.

## 4.0 QUANTITATIVE CHARACTERIZATION: QU-TUBES VS. HEAT PIPES

This chapter presents quantitative thermal characterizations of the Qu-Tube operations in comparison with the heat pipe operations, using an elaborate test stand connected to a state-of-the-art LabView DAQ system in a controlled environment. Section 4.1 provides more details on the experimental setup, while Section 4.2 presents experimental condition matrices representing the varied parameters. Section 4.3 presents basic performance data for the selected test articles (QT-2 and HP-2). For all of the test articles (QT-1, QT-2, HP-1 and HP-2), Section 4.4 presents comparative performance characterizations, including thermal loading input/output and detailed temperature profiles along the tube surfaces. Finally, Section 4.5 compares the measured effective thermal conductivities of the Qu-tubes with those of the heat pipes.

### 4.1 Experimental Set-Up Under a Controlled Environment

The experimental setup for the quantitative characterization of the test articles has been designed, constructed, and implemented in-house at the Facility for Innovative Research in Structures Technology (FIRST) (Fig. 12a & b). The test stand enables accurate setting of the predetermined orientation of the test articles, which are all 36 in. in length. The entire set up, including the test tube, the heater shoe (4 in. in length) containing 24 electrical heater elements, and the cooling jacket (4 in. in length) of coiled copper tubing, is wrapped in insulation and placed inside the 36 in. x36 in. x36 in. Cincinnati Sub-Zero (CSZ) environment control unit, which will be maintained at the heat sink coolant temperature (Fig. 12-c).

A data acquisition and control system has been developed to control the power provided to the heating elements and to monitor the temperature data from twelve (12) thermocouple probes placed along the adiabatic section of the heat pipe, from an additional five probes located at both ends of the test tube, and from the inlet/outlet locations of the coolant flow path in the condenser section, in addition to monitoring the environmental temperature (Fig. 13-a). The condenser coolant flow rate is detected by a digital turbine flow meter. All of the measured data are monitored, analyzed, and stored by the DAQ system (Fig. 13-b).

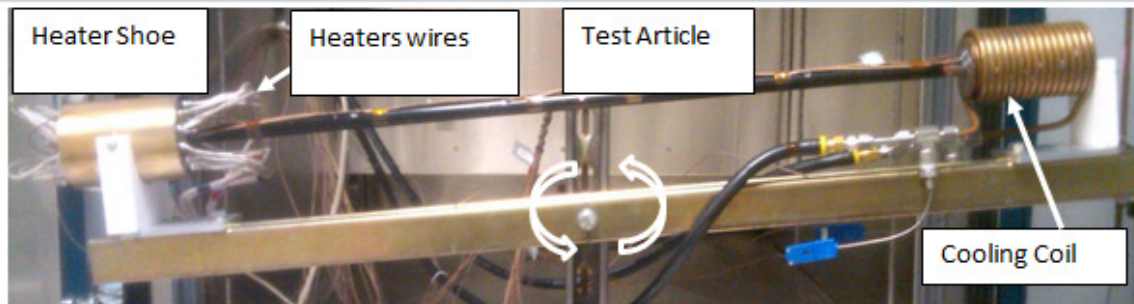
A number of necessary refinements and preparations have been conducted to facilitate the quantitative characterizations of the test articles. Three major tasks have been completed:

1. In order to meet the stringent requirements for accurate temperature measurements, all of the industry-standard thermocouple probes ( $\pm 1.0^{\circ}\text{C}$  measurement uncertainty) were calibrated by elaborate laboratory processes using the NIST standard probes to ensure  $\pm 0.1^{\circ}\text{C}$  uncertainties.

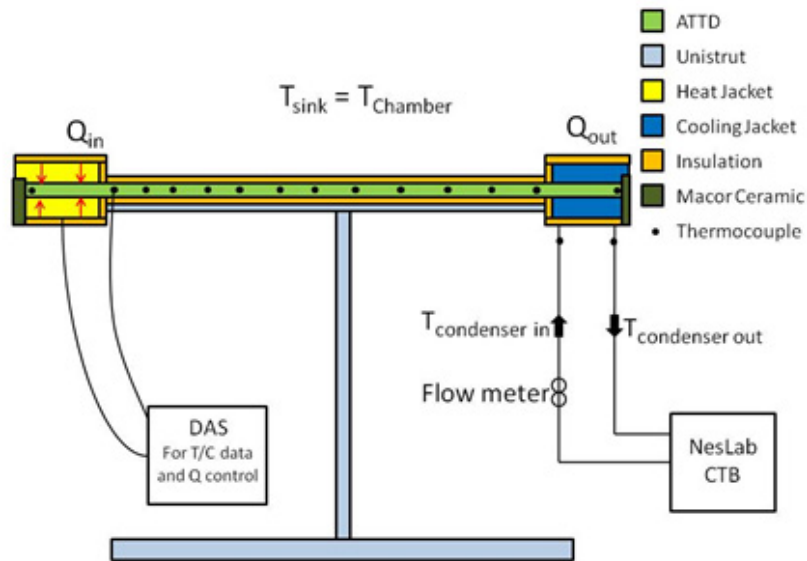
2. Accurate detection of the coolant flow rate was ensured by inputting the correct flow meter calibration numbers for the LabView VI DAQ program and maintaining the measurement uncertainty to  $\pm 2\%$ .
3. Noise in the thermocouple probe readings was found to be caused by cross-talk between the heater power electrical current and the thermocouple probe voltages when they were mounted on the test article surfaces, which were interfaced with the copper heater shoes via a pair of stainless steel inserts. The stainless inserts were replaced by MACOR, a glass ceramic material with an extremely high electrical resistance. Thus, MACOR acts as a highly effective insulator while still possessing a fairly acceptable thermal conductance, as shown in Table 3.

**Table 3: Heater Insert Material Properties**

Heater Insert Material	Thermal Conductivity (25°C)	Electrical Resistivity
304 Stainless Steel	16 W/m·K	$7.2 \times 10^{-3}$ Ohms/m
Glass Ceramic (MACOR)	1.4 W/m·K	$> 10^{19}$ Ohms/m



(a)

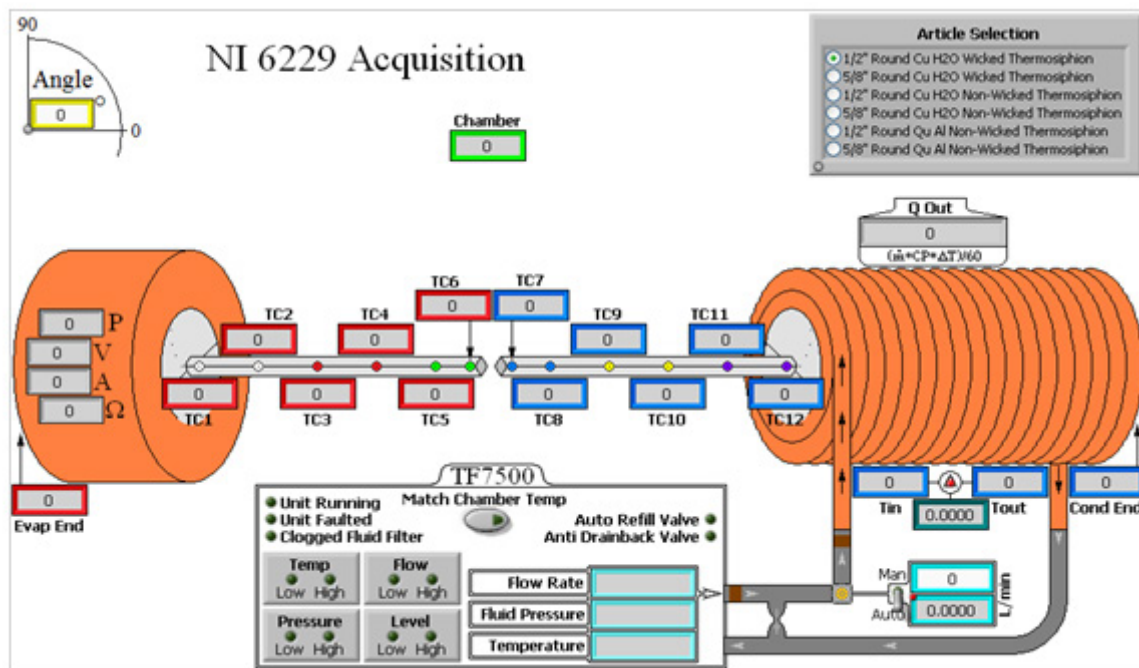


(b)

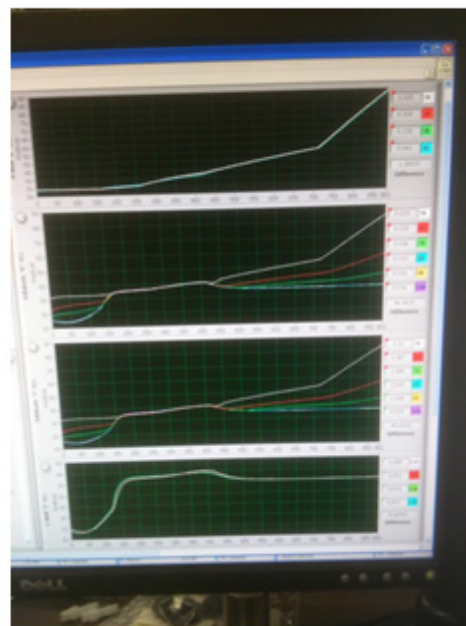
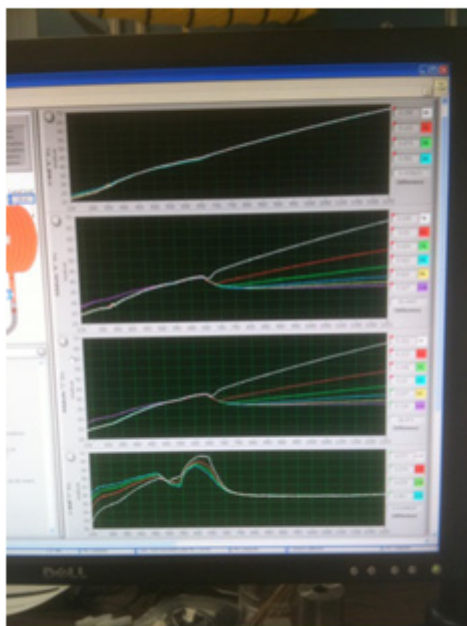


(c)

**Figure 12: Experimental Set-Up: (a) the Adjustable Inclination of the Test Article, (b) the Schematic of the Experimental Set-Up, and (c) the Cincinnati Sub-Zero (CSZ) Chamber**



(a)



(b)

**Figure 13: (a) Front-End Interface of the LabView VI Data Acquisition Program, and (b) Typical Readout Screens for the Thermocouple Temperature Data**

## 4.2 Experimental Test Matrices

The quantitative characterizations consider four parameters: the types of tubes, the coolant inlet temperatures to the condenser, the tilt angles of the test articles, and the DC heater power input. Tables 4 to 7 show experimental test matrices for HP-1, QT-1, HP-2 and QT-2, respectively. Each matrix presents parametric variations of three coolant temperatures (20°C, 40°C and 60°C), three tilt angles (+5, +1, and -5 degrees from the horizon), and the tested range of DC heater powers  $P_{\max}$ .

The positive tilt angle is designated when the evaporator is below the condenser and negative when the evaporator is above the condenser. The negative tilt angles, therefore, can drive most of the working fluid to move from the evaporator toward the condenser. This will result in instantaneous dry-out of the evaporator and unstable operation, even with a very low heater power input. For both types of tubes (Qu-tubes and heat pipes) with -5 degree inclinations, a steady state of thermal conditions was never reached, as expected, and an indication of dry-out occurred at an earlier stage of heating, as low as at  $P_{\text{in}} = 10\text{W}$ . Thus, no measurement data are available for the test cases with a -5 degree inclination.

Different maximum ranges of the input heater power were considered depending upon the individual experimental conditions. The maximum input power for the Qu-tube has to be kept substantially lower than that of the heat pipe operations. This is because the welding joint of the evaporator cap of the aluminum Qu-tube reaches a significantly earlier thermal breaching point when heated by the surrounding heater shoes (refer to Fig. 12), whereas the copper heat pipe has no welded cap and can thus be heated to a substantially higher temperature.

For each of the four test articles (QT-1, QT-2, HP-1 and HP-2), experiments are conducted by allowing parametric variations with respect to the reference condition of +5 degree tilt and  $T_{\text{coolant}} = 40^\circ\text{C}$ . First, the coolant temperature was varied ( $T_{\text{coolant}} = 20^\circ\text{C}$ ,  $40^\circ\text{C}$ , and  $60^\circ\text{C}$ ) while the tilt angle was fixed at +5 degrees. Then, the tilt angle (+1 degree and -5 degrees) are varied while  $T_{\text{coolant}} = 40^\circ\text{C}$  remained constant.

**Table 4: Test Matrix for the 36 in. (L) x 0.5 in. (D) Wicked Copper Heat Pipe (HP-1)**

Tilt Angle (°)	Coolant Temperature (°C)		
	20	40	60
1	No Tests	$P_{\max} = 700\text{W}$	No Tests
5	$P_{\max} = 700\text{W}$ Meta-stable fluctuations for $P_{\text{input}} = 40\text{W}$ to 180W.	$P_{\max} = 700\text{W}$ . Meta-stable fluctuations in temperature readings were observed for $P_{\text{input}} = 70\text{W}$ to 140W.	$P_{\max} = 700\text{W}$ Meta-stable fluctuations for $P_{\text{input}} = 60\text{W}$ to 70W.
-5	No Tests	Steady state was not reached, and a typical indication of dry-out occurred at $P_{\text{in}} = 10\text{W}$ and higher.	No Tests
*Water coolant flow rate was maintained at approximately 0.1 gpm. *Tilt angle is positive when the evaporator is below the condenser.			

**Table 5: Test Matrix for the 36 in. (L) x 0.5 in. (D) Aluminum Qu-Tube (QT-1)**

Tilt Angle (°)	Coolant Temperature (°C)		
	20	40	60
1	No Tests	No Tests	No Tests
5	$P_{\max} = 200\text{W}$	$P_{\max} = 250\text{W}$	$P_{\max} = 250\text{W}$ $P_{\max} = 200\text{W}$
-5	No Tests	$P_{\max} = 70\text{W}$	$P_{\max} = 70\text{W}$
*Water coolant flow rate was maintained at approximately 0.1 gpm. *Tilt angle is positive when the evaporator is below the condenser.			

**Table 6: Test Matrix for the 36 in. (L) x 5/8 in. (D) Wicked Copper Heat Pipe (HP-2)**

Tilt Angle (°)	Coolant Temperature (°C)		
	20	40	60
1	No Tests	$P_{\max} = 700W$ $T_{\max} = 129^{\circ}C$	No Tests
5	$P_{\max} = 700W$ $T_{\max} = 120^{\circ}C$	Operation becomes highly unstable at $P_{\max} > 450W$ and $T_{\max} = 107^{\circ}C$ . However, the repeated test does not show any noticeable instability, up to $P_{\max} = 600W$ .	$P_{\max} = 700W$ $T_{\max} = 132^{\circ}C$
-5	No Tests	Steady state was not reached, and a typical indication of dry-out occurred at $P_{\max} = 20W$ or higher.	No Tests
<p>*<math>T_{\max}</math> was determined from the average of the adiabatic temperature readings.</p> <p>*Water coolant flow rate was maintained at approximately 0.1 gpm.</p> <p>*Tilt angle is positive when the evaporator is below the condenser.</p>			

**Table 7: Test Matrix for the 36 in. (L) x 5/8 in. (D) Aluminum Qu-Tube (QT-2)**

Tilt Angle (°)	Coolant Temperature (°C)		
	20	40	60
1	No Tests	$P_{\max} = 150W$	No Tests
5	$P_{\max} = 300W$	$P_{\max} = 320W$ <i>No signs of unstable operation were detected.</i>	$P_{\max} = 160W$
-5	No Tests	$P_{\max} = 50W$ <i>Unstable operation/possible dryout was observed.</i>	No Tests
<p>*Water coolant flow rate was maintained at approximately 0.1 gpm.</p> <p>*Tilt angle is positive when the evaporator is below the condenser.</p>			

### 4.3 Basic Performance Test: Qu-Tubes vs. Heat Pipes

Basic performance data are presented for the 5/8"-diameter Qu-tube (QT-2) and for the 5/8"-diameter heat pipe (HP-2) in Figures 14 to 16. These data include the axial temperature distributions in the adiabatic sections for the range of heat input powers (Fig. 14), q-T curves (Fig. 15-a, Fig. 16-a), and the ratio of heat loss to the heat input power (Fig. 15-b, Fig. 16-b).

The axial temperature distributions at different heat input powers show a gradual gradient along the tube wall of the adiabatic section, from the evaporator to the condenser (Fig. 14). Both QT-2 and HP-2 show similar slight temperature gradients in the adiabatic sections. This indicates that the two test articles respond to the thermal loads similarly as a passive heat pipe.

In Figures 15 and 16, the heat removed through the coolant flow at the condenser is determined from the calorimetric energy balance, i.e.,

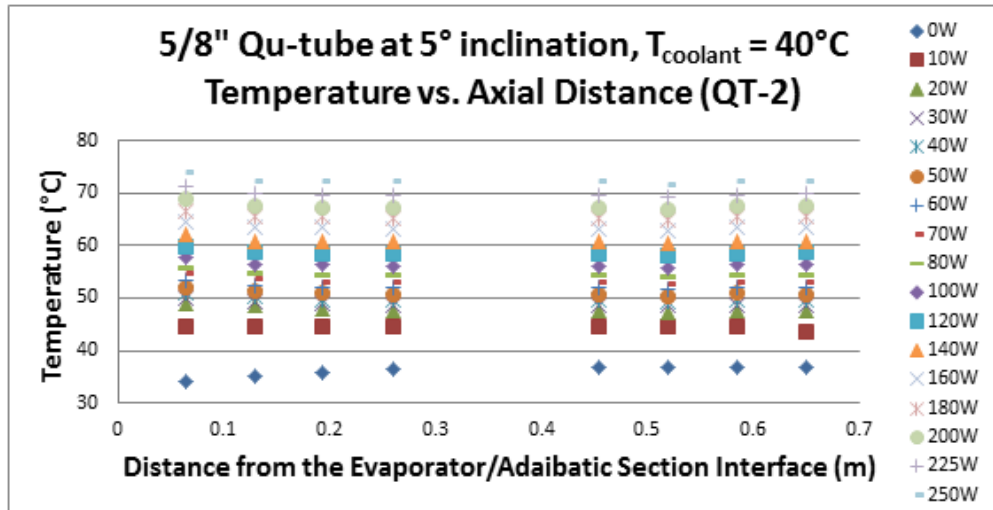
$$q_{out} = (\dot{m}c_p\Delta T)_{coolant} \quad (3-1)$$

where  $\dot{m}$  is the coolant mass flow rate in g/s,  $c_p$  denotes the specific heat of the coolant water in J/g·K, and  $\Delta T$  is the temperature differential between the coolant inlet and outlet in K. The heat loss to the environment ( $q_{loss}$ ) is calculated as the DC heater power input ( $q_{in}$ ) minus the heat taken away from the condenser ( $q_{out}$ ), i.e.,

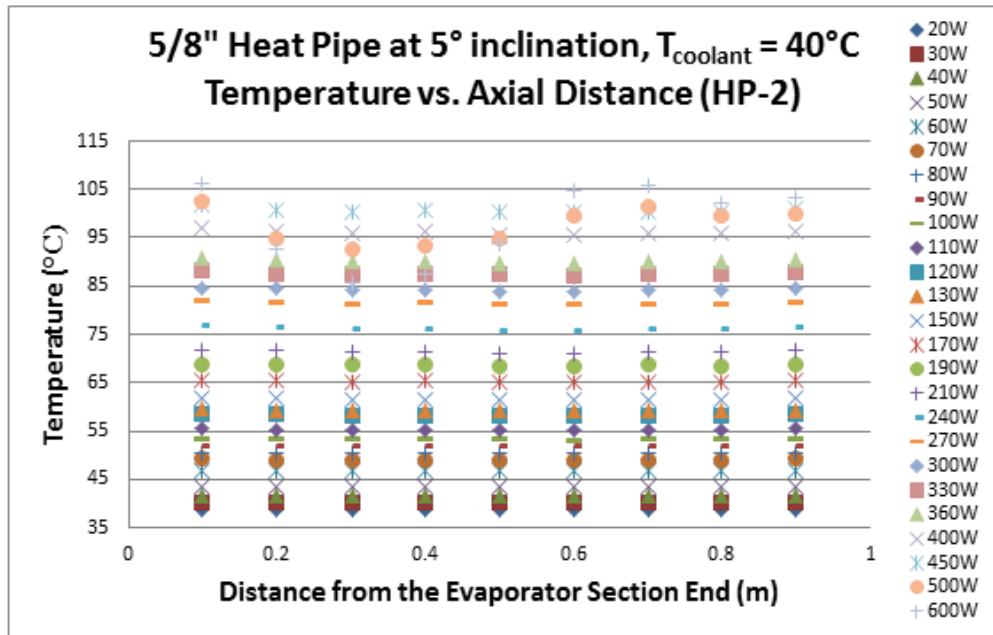
$$q_{loss} = q_{in} - q_{out} \quad (3-2)$$

Both QT-2 and HP-2 show a positive, nearly linear relationship between the time-averaged  $q_{out}$  and the average adiabatic section temperature (Fig. 15-a, Fig. 16-a). The maximum adiabatic temperature for the Qu-tube must be kept substantially lower than that of the heat pipe operations. As previously stated, this is because the welding joint of the evaporator cap of the aluminum Qu-tube reaches its thermal breaching point significantly earlier than the copper heat pipe's which does not have a welded cap. This also lowers the range of the maximum heat removed from the Qu-tube's condenser, in comparison with the heat pipe's.

The heat loss increases as a function of heat input for both test articles (Fig. 15-b, Fig. 16-b). Both QT-2 and HP-2 show an approximately 40% heat loss to the external environment from the total input power. The uncertainty of temperature readings from the thermocouple probes is within  $\pm 0.1^\circ\text{C}$ ; of the digital flow meter readings is within  $\pm 2\%$ ; and of the measured heat input is within  $\pm 1\%$ . Note that these tight ranges of measurement uncertainties keep the error bars within the symbol sizes depicted in the plots.

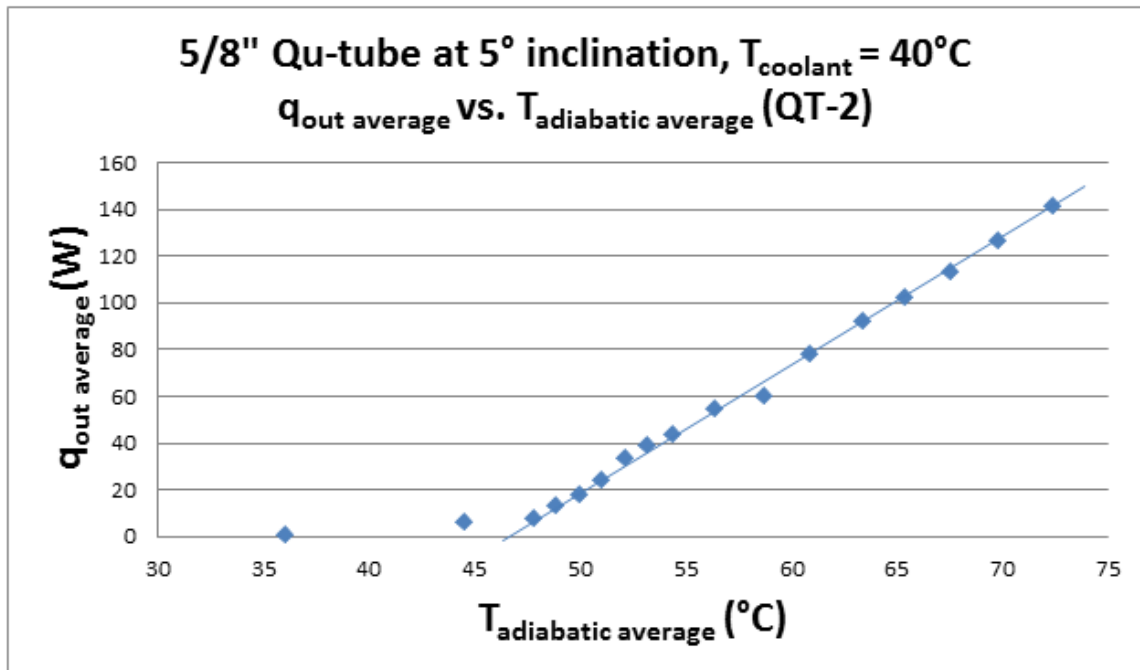


(a)

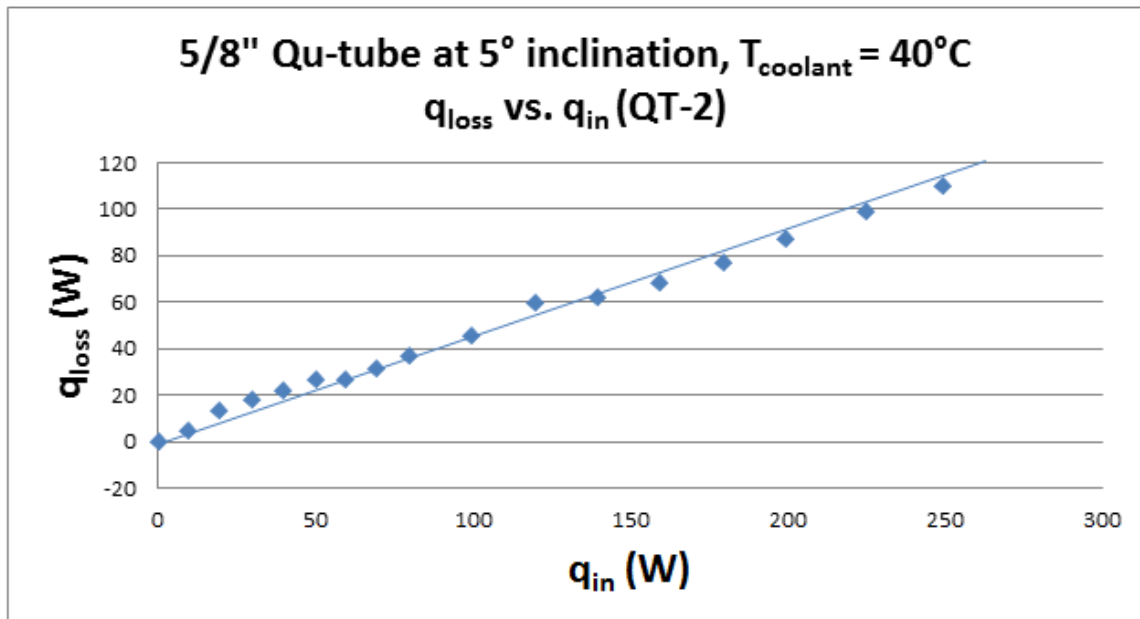


(b)

**Figure 14: Axial Temperature Distributions for the Adiabatic Regions**

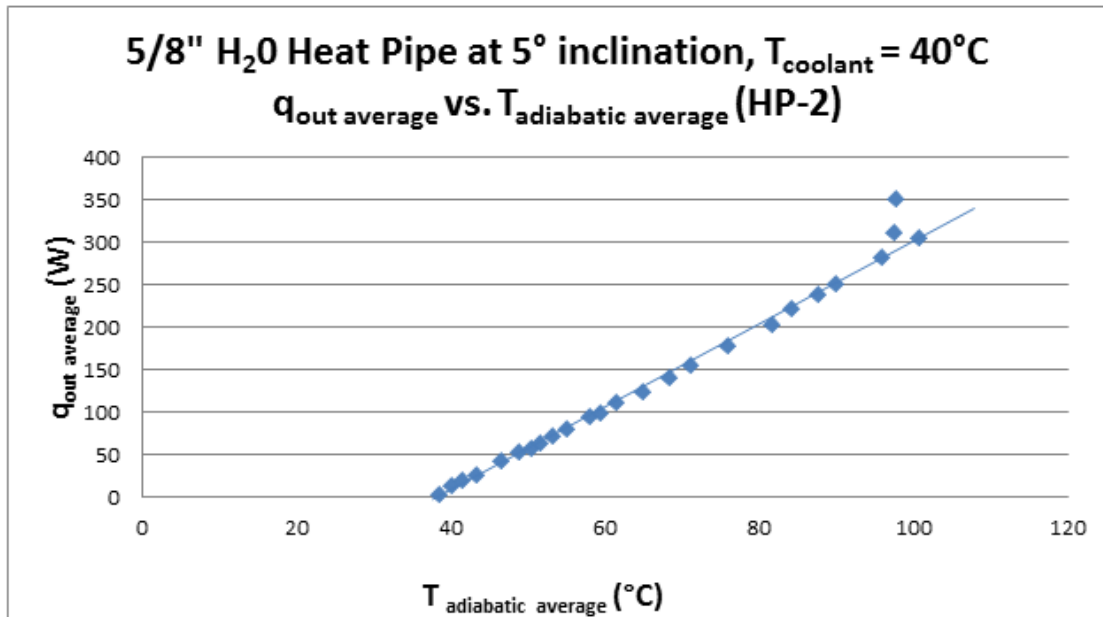


(a)

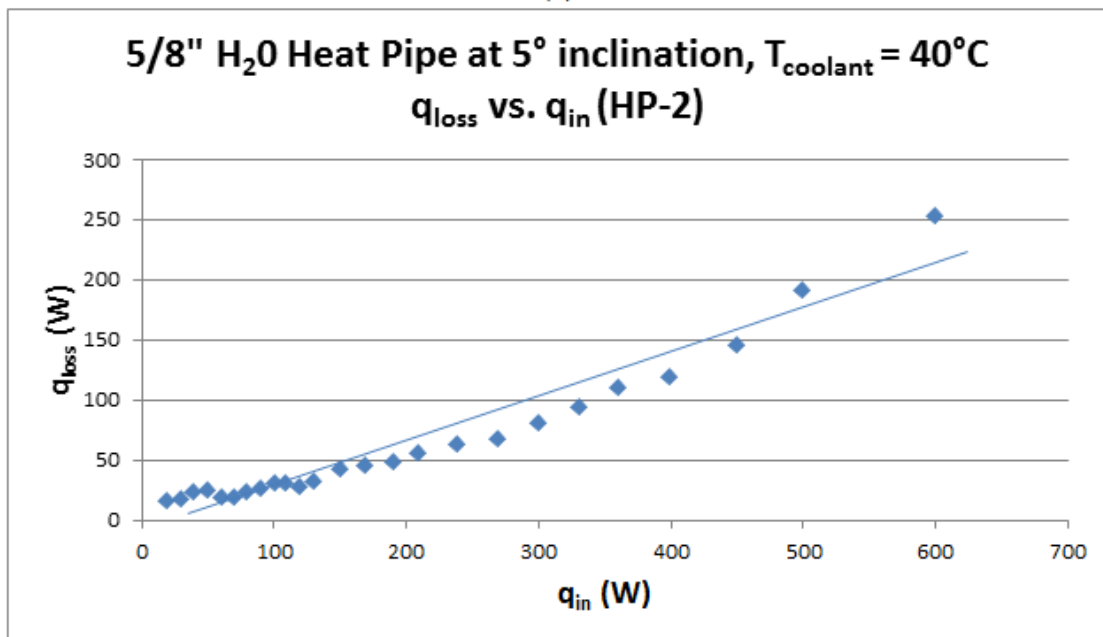


(b)

**Figure 15: Basic Performance Data for the 5/8 in. Qu-Tube (QT-2)**



(a)



(b)

**Figure 16: Basic Performance Data for the 5/8 in. Heat Pipe (HP-2)**

#### 4.4 Comparative Thermal Performance: Qu-Tubes vs. Heat Pipes

Figures 17 to 24 present comparative performance curves for Qu-tubes (QT-1 & QT-2) vs. heat pipes (HP-1 & HP-2) for the measured heat amounts of heat removed from the condenser ( $q_{out}$ ) with increasing heat input ( $q_{in}$ ). The x-axis indicates the elapsed time with a time scale bar that is independently defined for each figure. While  $q_{in}$  increases stepwise in fixed increments,  $q_{out}$  shows time-varying values for all of the tested cases. This is believed to be because the thermal transport behaviors inside the tubes are not perfectly steady but instead vary in time, thus causing the thermal loadings to fluctuate.

Three primary temperatures are also presented in Figures 17 to 24: the evaporator temperature ( $T_{evap}$ ) which is taken from the TC probe located at the evaporator end (refer to Fig. 132-a); the adiabatic temperature ( $T_{adia}$ ), which is averaged from thermocouple readings TC2 to TC 11; and the condenser temperature ( $T_{cond}$ ), which is obtained from the mean of TC12 and the TC probe located at the condenser end. After allowing the tube to reach steady state at a new stepwise DC heat input power, the temperatures ( $T_{evap}$ ,  $T_{adia}$  &  $T_{cond}$ ) were recorded. Because they look like step functions, these can be called “quasi-steady” conditions. Table 8 summarizes the test parameters for each of the plots: four different tube types (QT-1, QT-2, HP-1 & HP-2), two inclination angles (+5 degrees & +1 degree, both with condenser above evaporator and gravity assisted), and three coolant inlet temperatures (20°C, 40°C & 60°C).

**Table 8: Test Parameters for Figures 17 to 24**

Tube Type	Figure Number	Tilt Angle (degrees)	Coolant Temperature (°C)
<b>½ in. Qu-Tube vs. ½ in. Heat Pipe (QT-1 vs. HP-1)</b>	Fig. 17	+5	40
	Fig. 18	+5	20
	Fig. 19	+5	60
	Fig. 20	+1	40
<b>5/8 in. Qu-Tube vs. 5/8 in. Heat Pipe (QT-2 vs. HP-2)</b>	Fig. 21	+5	40
	Fig. 22	+5	20
	Fig. 23	+5	60
	Fig. 24	+1	40

The fundamental findings obtained from the comparative performance depicted in Figures 17 to 24 are as follows:

- $T_{\text{evap}}$  can be substantially higher than  $T_{\text{adia}}$ , and  $T_{\text{adia}}$  is generally higher than the fixed coolant inlet temperature,  $T_{\text{coolant}}$ .
- $T_{\text{adia}}$  of the Qu-tubes is consistently higher than  $T_{\text{adia}}$  of the heat pipes under an identical  $q_{\text{in}}$ . This agrees with the previous qualitative findings from the IR thermometry in Chapter 2. Indeed, this is a very important quantitative finding, since this may imply that the Qu-tubes run at higher operation temperatures and at lower thermal efficiencies, i.e., lower effective thermal conductivities than the heat pipes.
- Common to both the Qu-tubes and heat pipes, an increase of  $T_{\text{cond}}$  from 20°C to 60°C increases  $T_{\text{adia}}$  proportionally, whereas  $T_{\text{evap}}$  remains nearly unchanged. However, the amount of increase in  $T_{\text{adia}}$  with increasing  $T_{\text{cond}}$  is less pronounced for the Qu-tubes.
- While  $q_{\text{in}}$  increases substantially,  $T_{\text{cond}}$  does not show any dramatic increase from the constant coolant inlet temperature. However,  $T_{\text{cond}}$  of the Qu-tubes remains more stable and less susceptible to increasing  $q_{\text{in}}$ , i.e.,  $T_{\text{cond}}$  of QT-1 and QT-2 is less prone to increase with increasing  $q_{\text{in}}$  than  $T_{\text{cond}}$  of HP-1 and HP-2.

- The tilt angle change from +5 to +1 degrees does not show any pronounced difference in their operations for either of the Qu-tubes or the heat pipes, except for slight increase in  $T_{adia}$ , which may have occurred simply because of the slightly lowered gravity-assisted return of the condensed working fluid resulting in lower cooling efficiencies.
- The ratio of  $q_{out} / q_{in}$  shows a weak dependence on  $T_{coolant}$  showing a gradual increase with increasing coolant temperature, but this dependence is not fully consistent in all of the tested cases. More importantly, the  $q_{out} / q_{in}$  ratios of the Qu-tubes seems to be lower than those of the heat pipes. This implies that the cooling efficiencies of the former may be less than that of the latter. However, confirmation of this observation is postponed until the next section, in which the effective thermal conductivities ( $k_{eff}$ ) are presented and compared for the two test articles.

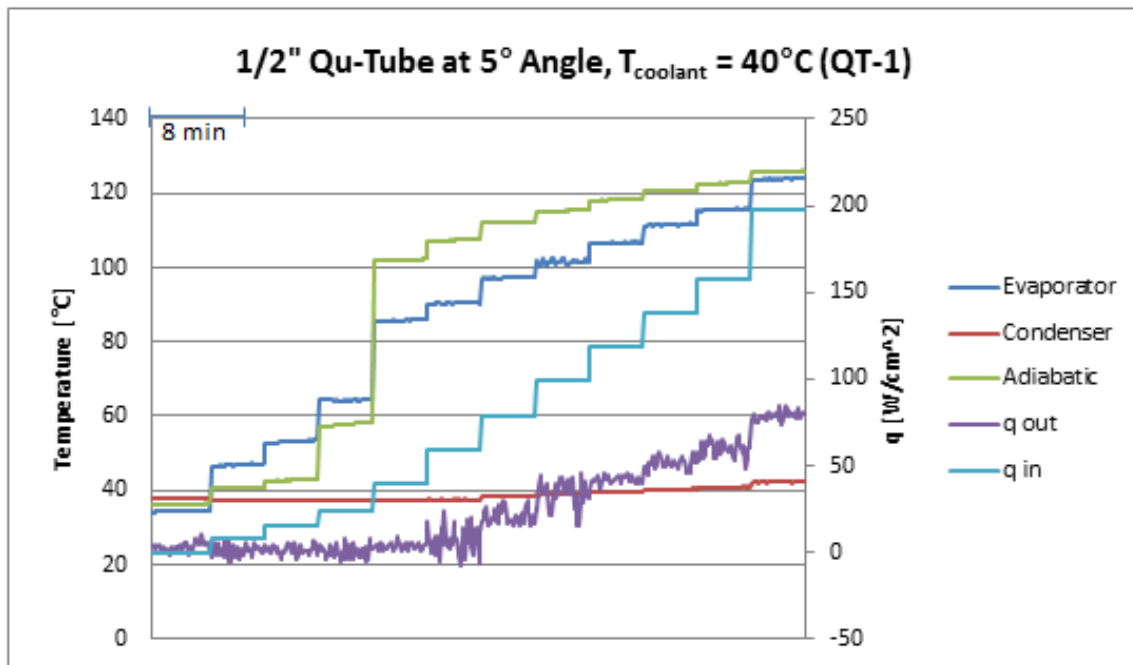
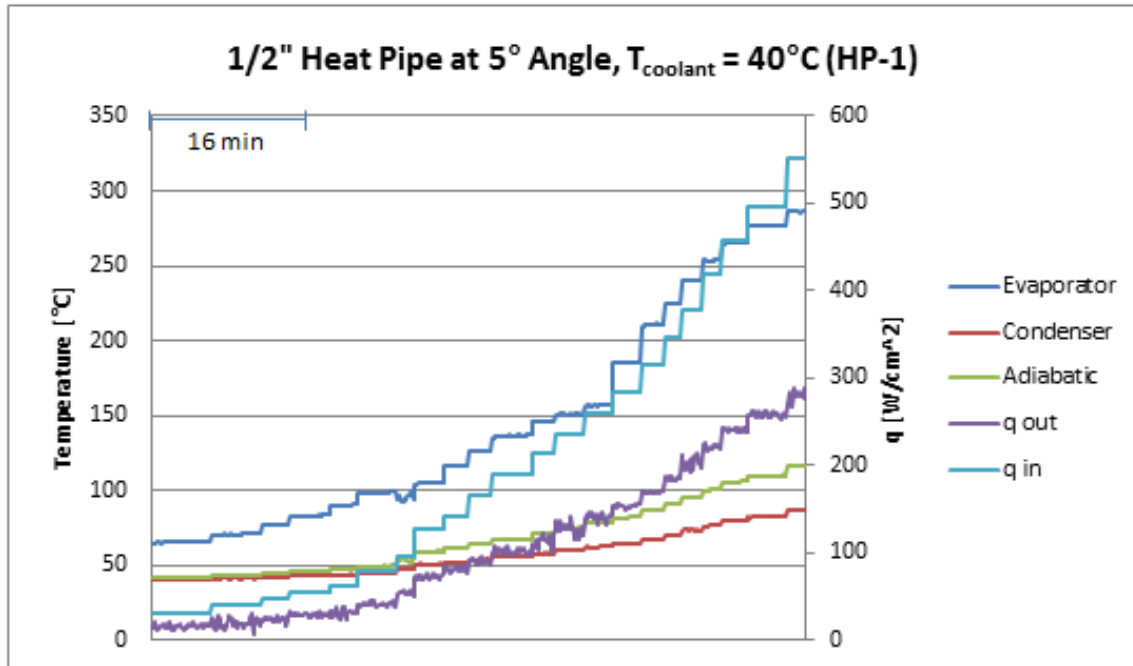


**Figure 17: Time History of Temperature Distributions and Heat Input/Output at Inclination Angle of +5 deg. (Condenser Upward) and Coolant Temperature of 40°C**

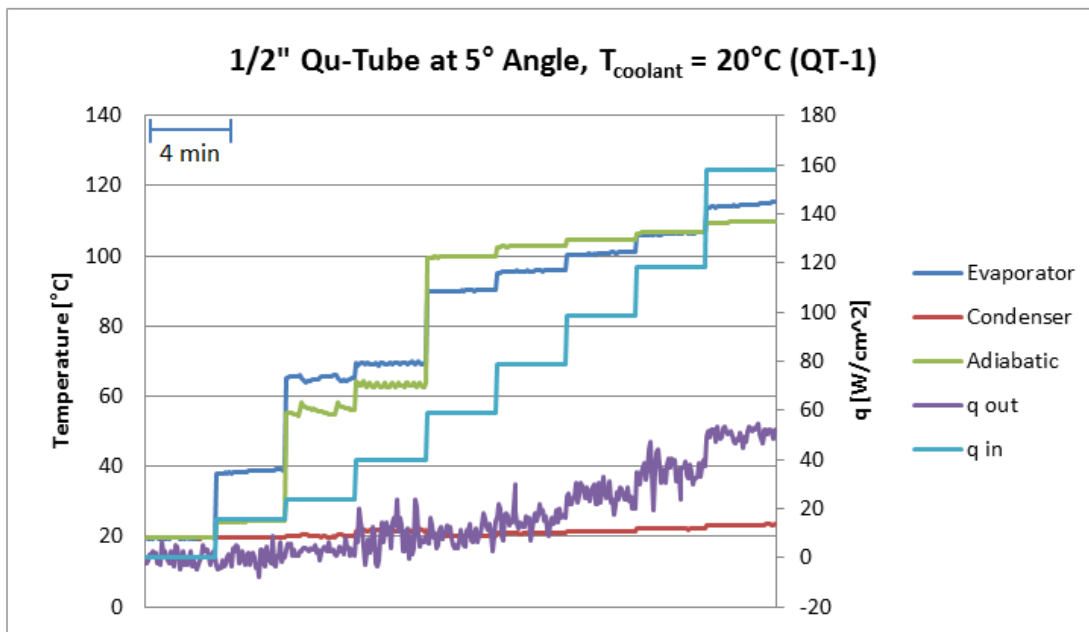
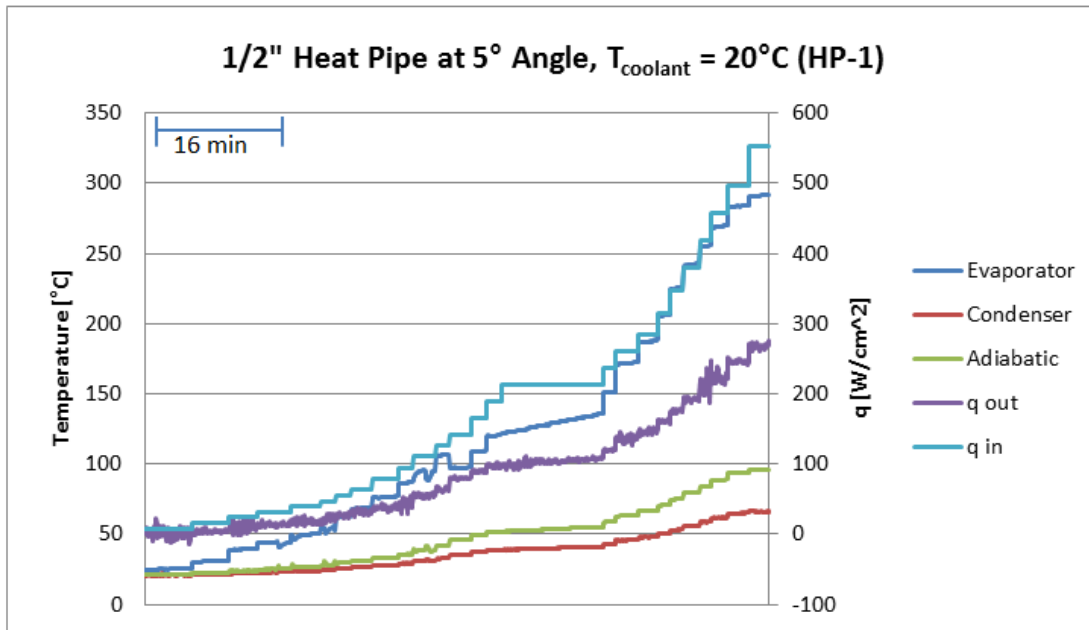
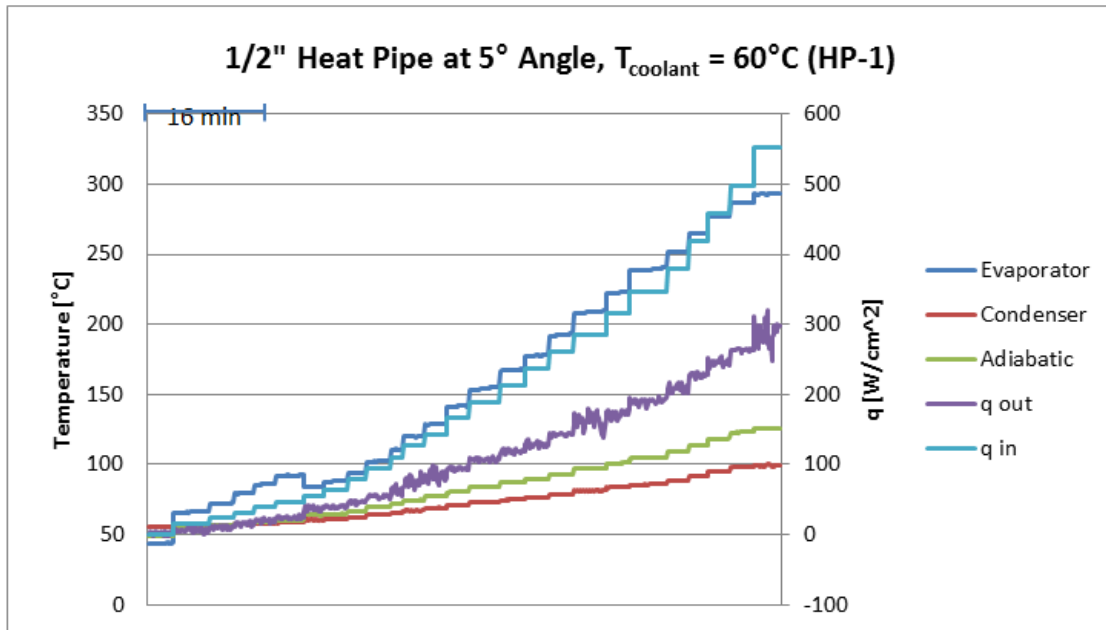
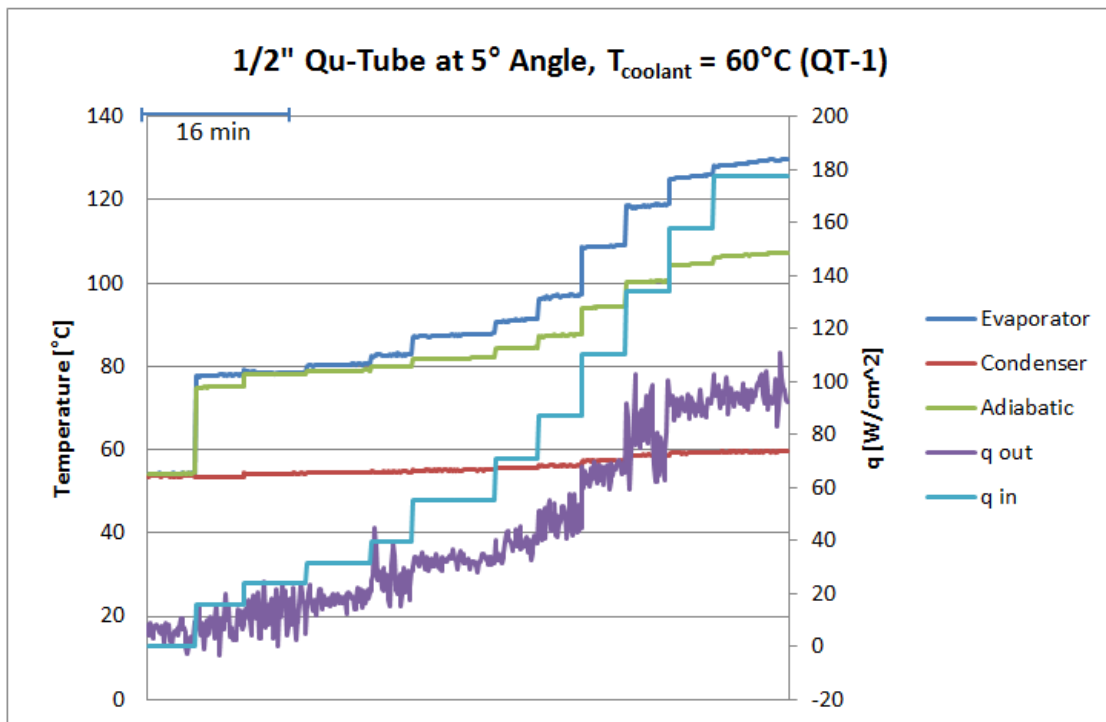


**Figure 18: Time History of Temperature Distributions and Heat Input/Output at Inclination Angle of +5 Degrees (Condenser Upward) and Coolant Temperature of 20°C**



(a)



(b)

**Figure 19: Time History of Temperature Distributions and Heat Input/Output at Inclination Angle of +5 Degrees (Condenser Upward) and Coolant Temperature of 60°C**

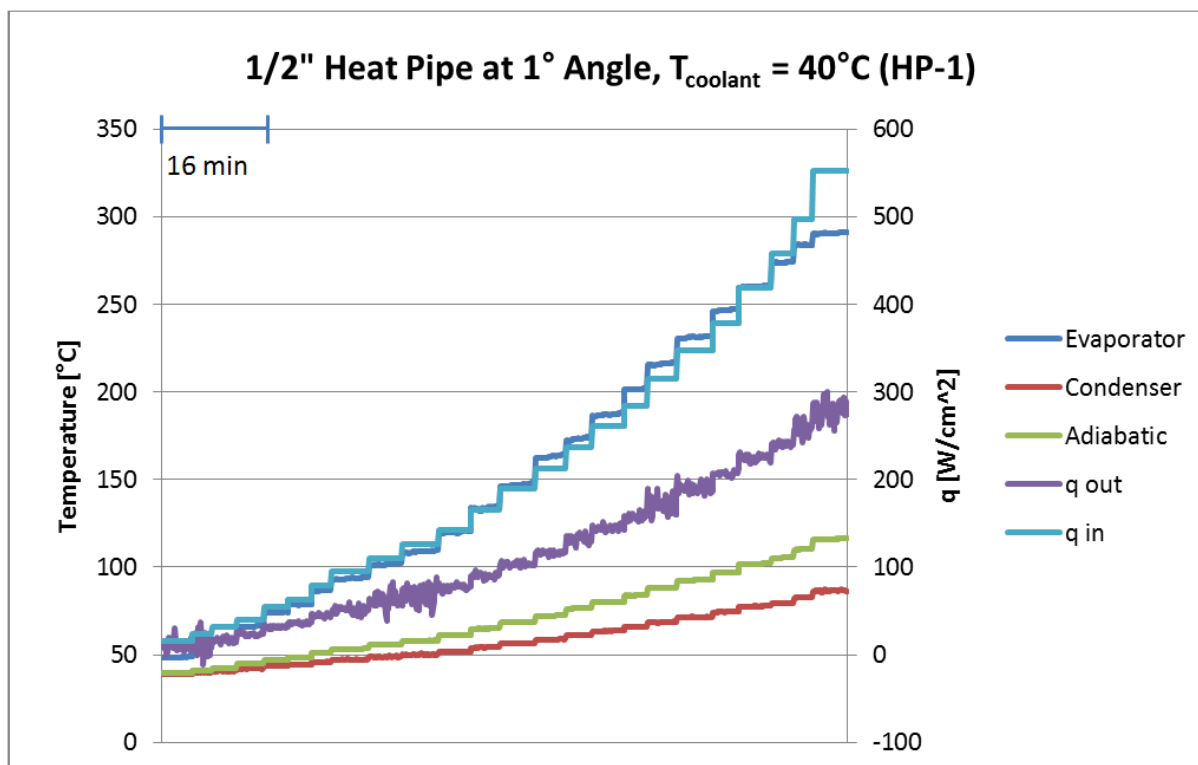


**Figure 20: Time History of Temperature Distributions and Heat Input/Output at Inclination Angle of +1 Degree (Condenser Upward) and Coolant Temperature of 40°C**

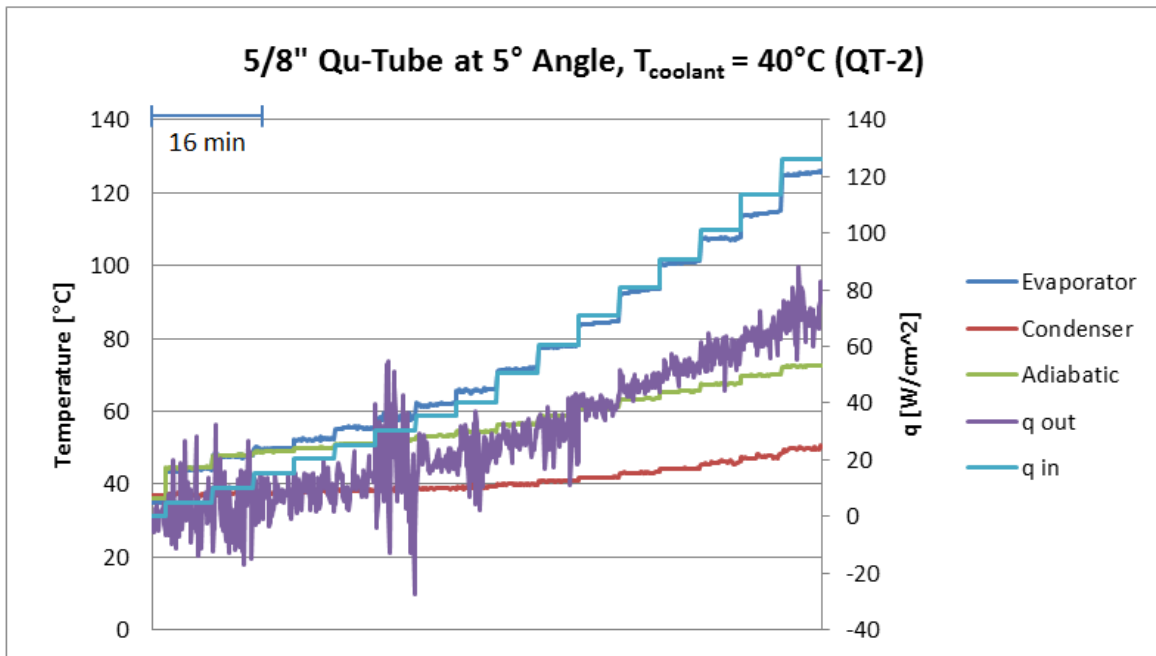
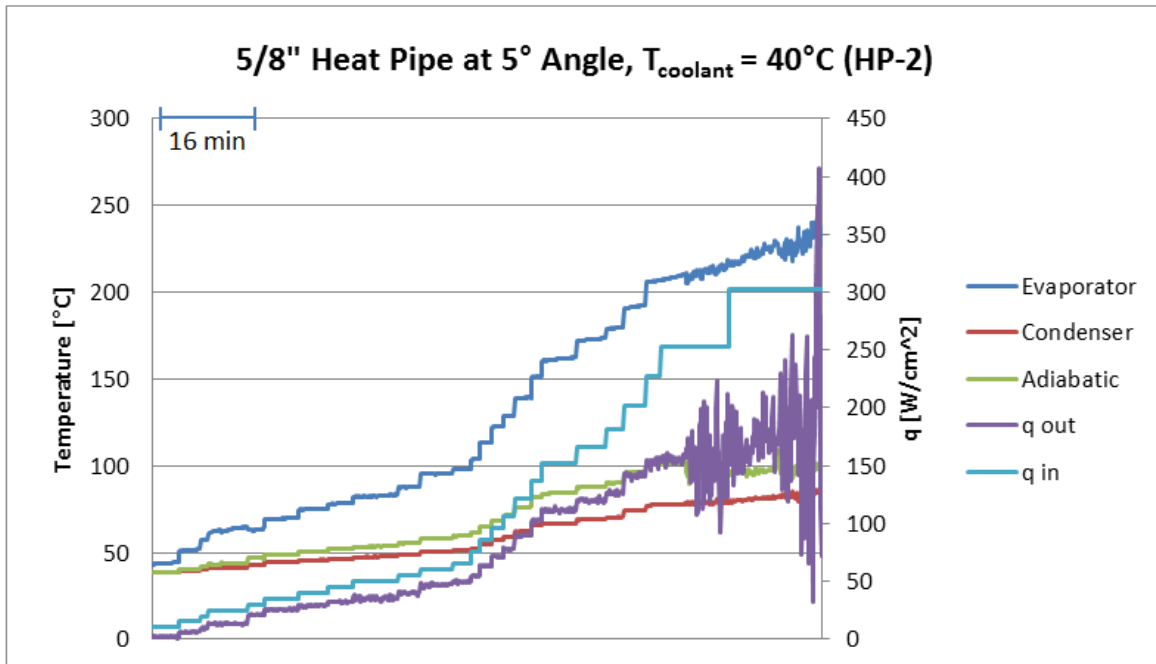


**Figure 21: Time History of Temperature Distributions and Heat Input/Output at Inclination Angle of +5 Degrees (Condenser Upward) and Coolant Temperature of 40°C**

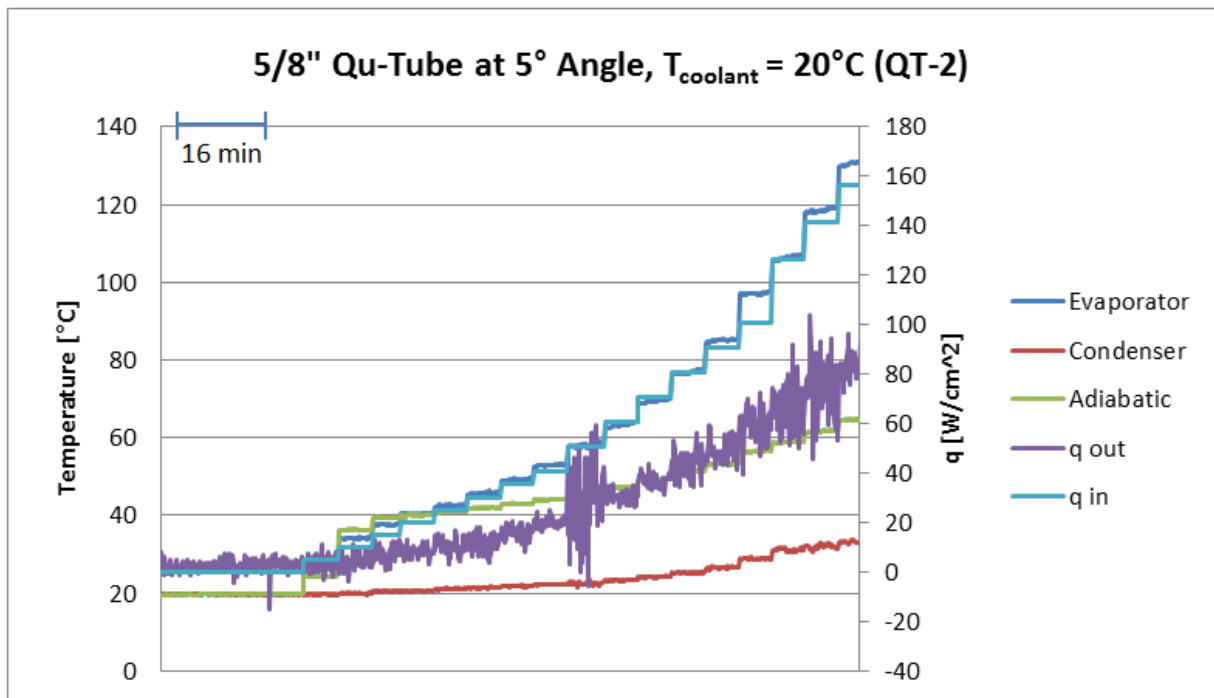
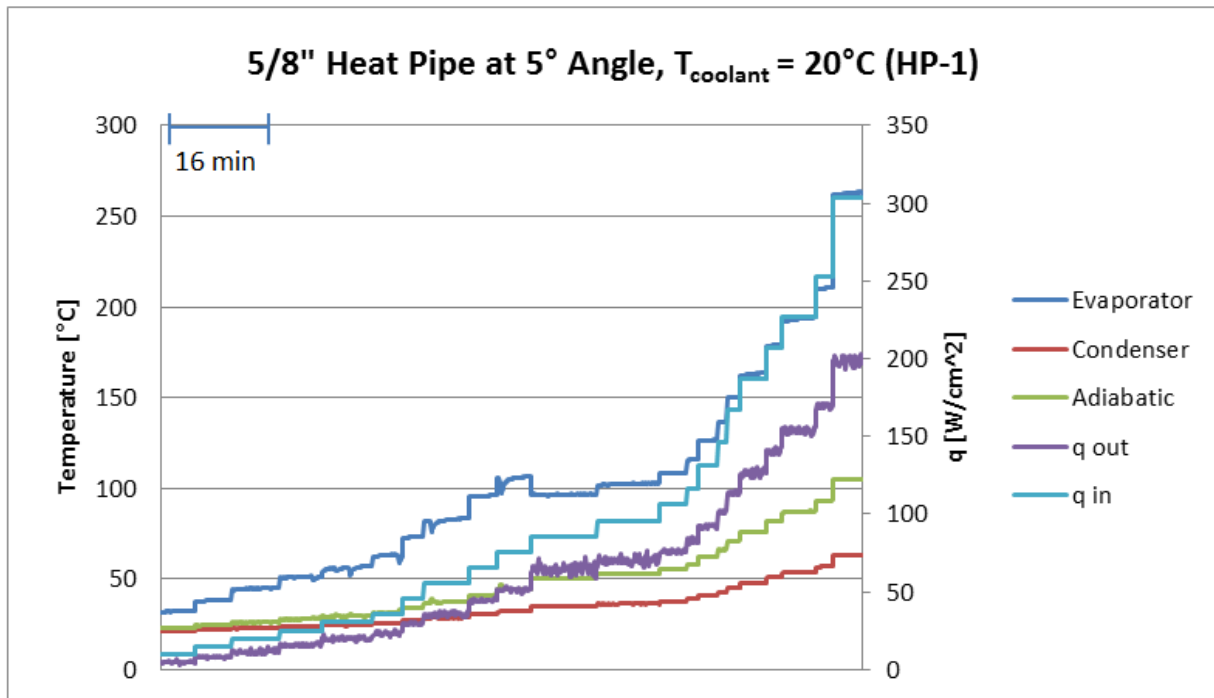


**Figure 22: Time History of Temperature Distributions and Heat Input/Output at Inclination Angle of +5 Degrees (Condenser Upward) and Coolant Temperature of  $20^{\circ}\text{C}$**

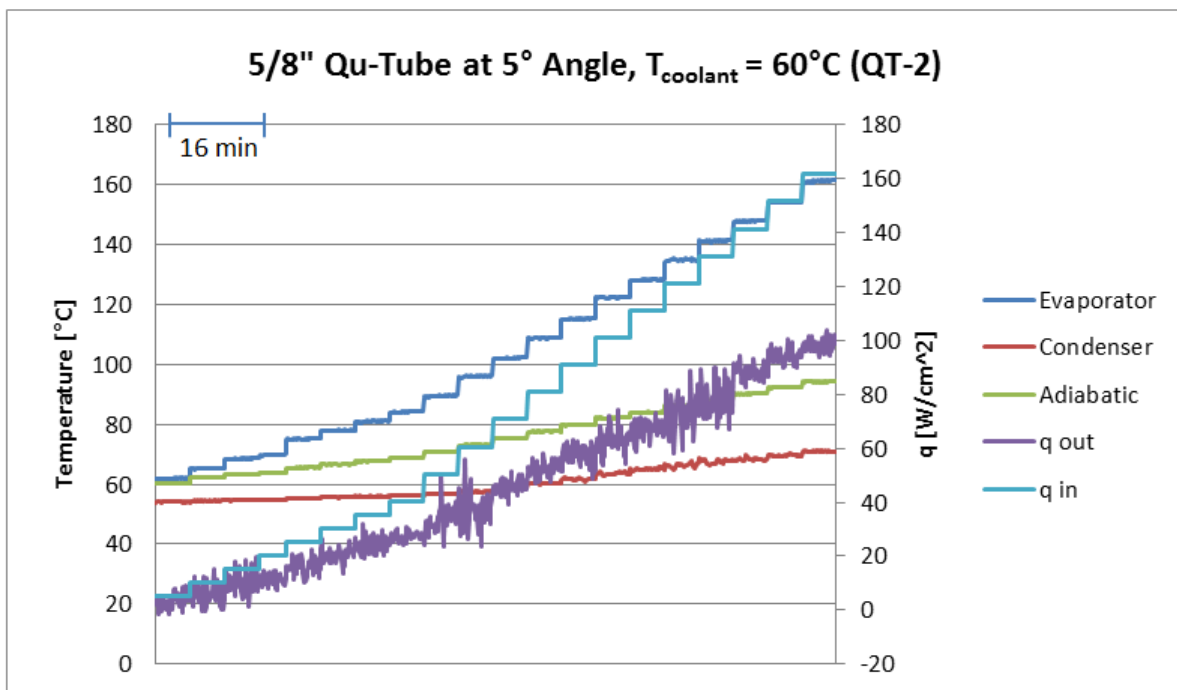
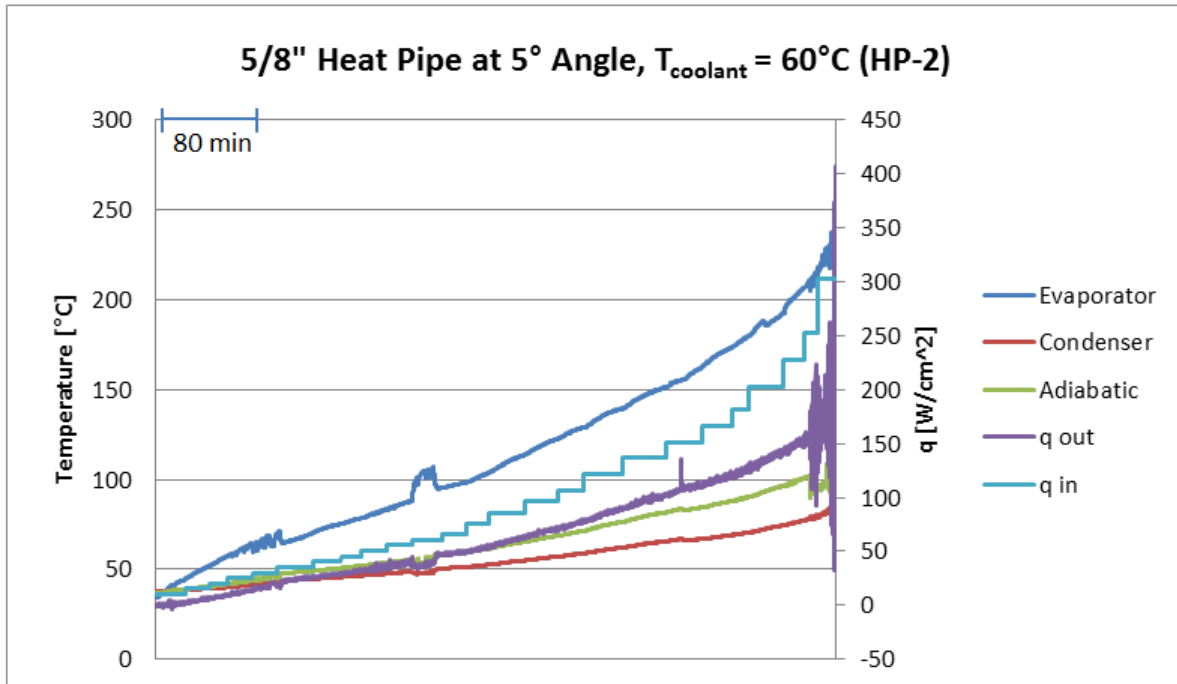


**Figure 23: Time History of Temperature Distributions and Heat Input/Output at Inclination Angle of +5 Degrees (Condenser Upward) and Coolant Temperature of 60°C**

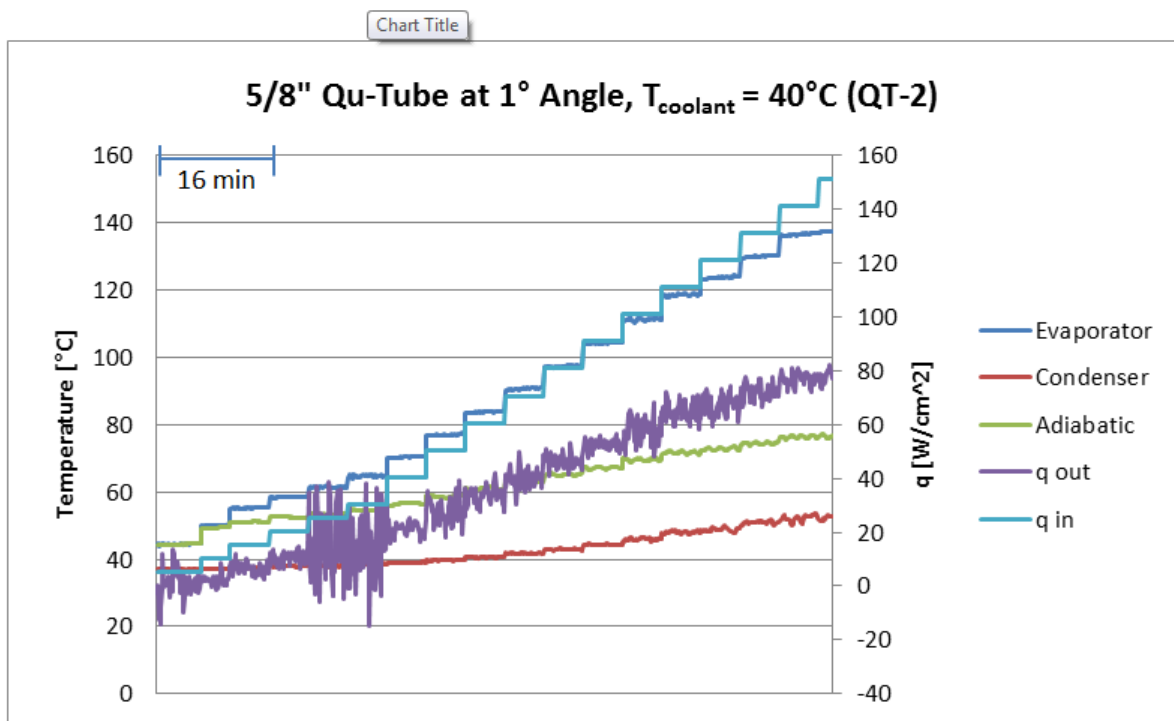
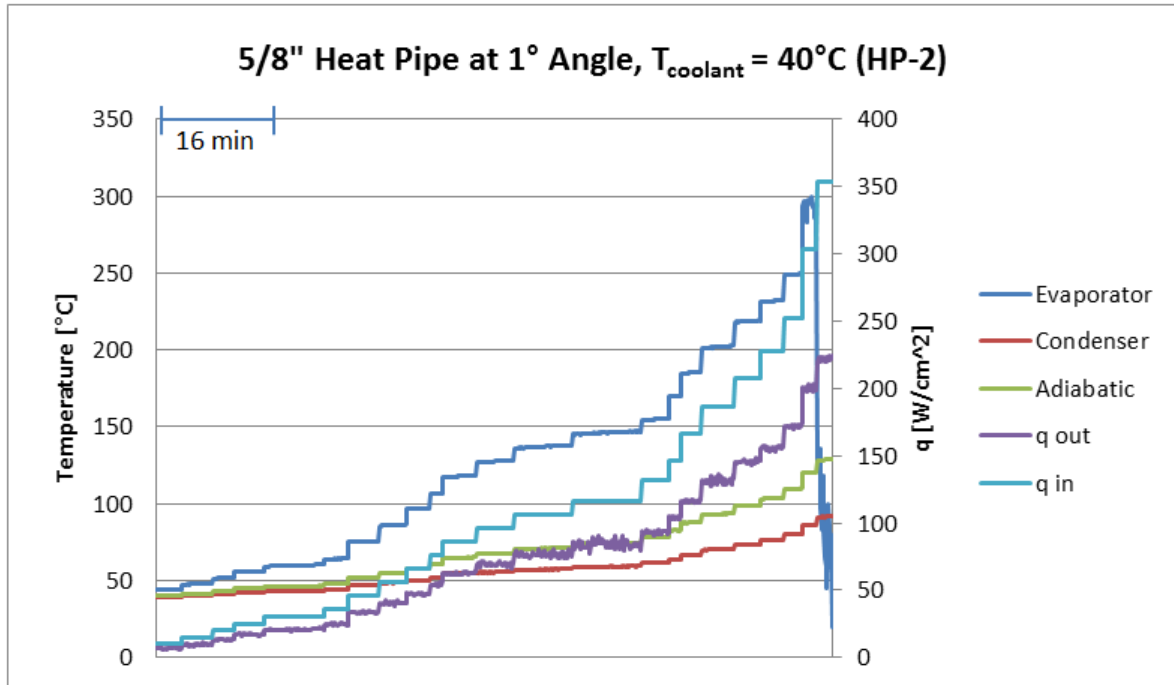


**Figure 24: Time History of Temperature Distributions and Heat Input/Output at Inclination Angle of +1 Degree (Condenser Upward) and Coolant Temperature of 40°C**

#### 4.5 Effective Thermal Conductivities: Qu-Tubes vs. Heat Pipes

Figures 25 to 32 show the effective thermal conductivities as functions of the heat removed by the coolant per unit cross-sectional area,  $Q / A$ . The effective thermal conductivities are calculated from the measured thermal data as follows:

$$k_{eff} = \frac{Q}{A} \cdot \frac{l_{eff}}{T_E - T_C} \quad (3-3)$$

$Q$ : Net heat transfer amount taken out through the condenser coolant

$A$ : Cross-sectional area of the tube

$l_{eff}$ :  $l_{eff} = (l_{evaporator} + l_{condenser}) / 2 + l_{adiabatic}$  [32 inches or 0.8128 m]

$T_E$ : Evaporator temperature average =  $(TC_{Evaporator\ end} + TC1) / 2$

$T_C$ : Condenser temperature average =  $(TC12 + TC_{Condenser\ end}) / 2$

TC1: the probe located at the beginning of the adiabatic section

TC12: the probe located at the end of the adiabatic section

Table 9 summarizes the test parameters for each of the plots: four different tube types (QT-1, QT-2, HP-1 & HP-2), two inclination angles (+5 & +1 degrees, both with the condenser upward with gravity assisted), and three coolant inlet temperatures (20°C, 40°C & 60°C).

**Table 9: Test Parameters for Figures 25 to 32**

Tube Type	Figure Number	Tilt Angle (degrees)	Coolant Temp. (°C)
<b>½ in. Qu-Tube vs. ½ in. Heat Pipe (QT-1 vs. HP-1)</b>	Fig. 25	+5	40
	Fig. 26	+5	20
	Fig. 27	+5	60
	Fig. 28	+1	40
<b>5/8 in. Qu-Tube vs. 5/8 in. Heat Pipe (QT-2 vs. HP-2)</b>	Fig. 29	+5	40
	Fig. 30	+5	20
	Fig. 31	+5	60
	Fig. 32	+1	40

The fundamental findings obtained from the comparisons of effective thermal conductivities of the Qu-tubes and the heat pipes, as depicted in Figures 25 to 32, are follows:

- The maximum heat fluxes removed ( $Q/A$ ) with the Qu-tubes are substantially lower than those of heat pipes. As previously stated, this is because the maximum heater power inputs of the Qu-tubes must be substantially lower than that of the heat pipes in order to prevent thermal breaching of the welding joint of the aluminum-made Qu-tube caps.
- In general, the effective thermal conductivity  $k_{\text{eff}}$  increases with increasing  $Q/A$  up to a certain value of  $Q/A$  to reach a maximum, after which it tends to remain constant. The constant value of  $k_{\text{eff}}$  can be considered as a measure of the characteristic heat removal efficiency for each of the test articles.
- The maximum values of  $k_{\text{eff}}$  for the Qu-tubes were measured to be less than 15,000 W/m·K, and approximately 35 times that of copper. There is one exceptional case for the ½-inch Qu-tube (QT-1) with  $T_{\text{coolant}} = 60^{\circ}\text{C}$  and a +5 degree tilt that provides a maximum  $k_{\text{eff}}$  of approximately 20,000 W/m·K (Fig. 27). In contrast, for the heat pipes, the maximum  $k_{\text{eff}}$  ranges from 15,000 W/m·K to 20,000 W/m·K. This implies that the Qu-tube operations are in general less efficient than the heat pipe, i.e., both  $k_{\text{eff}}$  and  $Q/A$  are lower for the Qu-tubes than for the heat pipes.
- A maximum of 15,000 W/m·K was also measured for similar Qu-tubes by Leland et al. of the AFRL Propulsion Directorate as shown in their 2011 report, AFRL-RZ-WP-TP-2011-

2078 [4]. The maximum  $k_{\text{eff}}$  values of 15,000 W/m·K of the Qu-tubes are far below the claimed number of 3,000,000 W/m·K in US Patent 6,132,823.

- Dependence of  $k_{\text{eff}}$  on tilt angle is weak, at best. The tilt angle change from +5 to +1 degrees shows slight reductions in  $k_{\text{eff}}$  for both the Qu-tubes and the heat pipes. However, the amounts of reduction are not very significant.

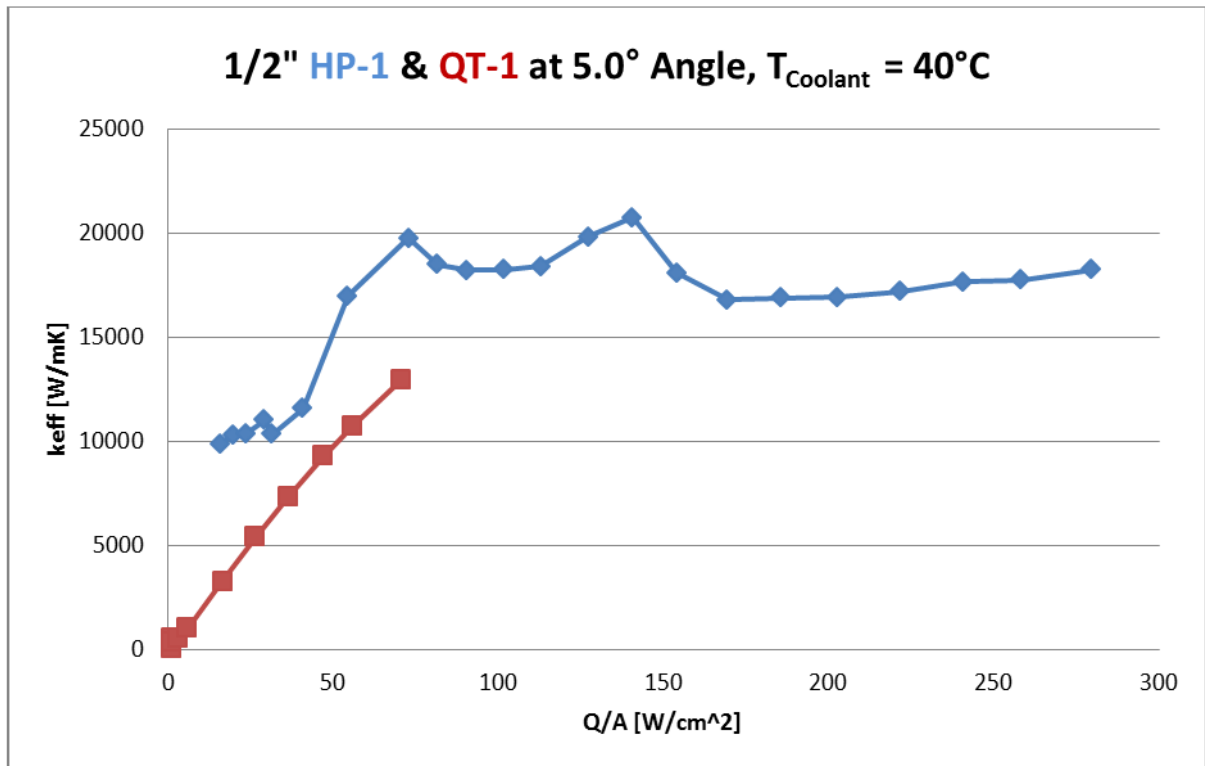


**Figure 25: Effective Thermal Conductivity at Inclination Angle of +5 Degrees (Condenser Upward) and Coolant Temperature of 40°C**

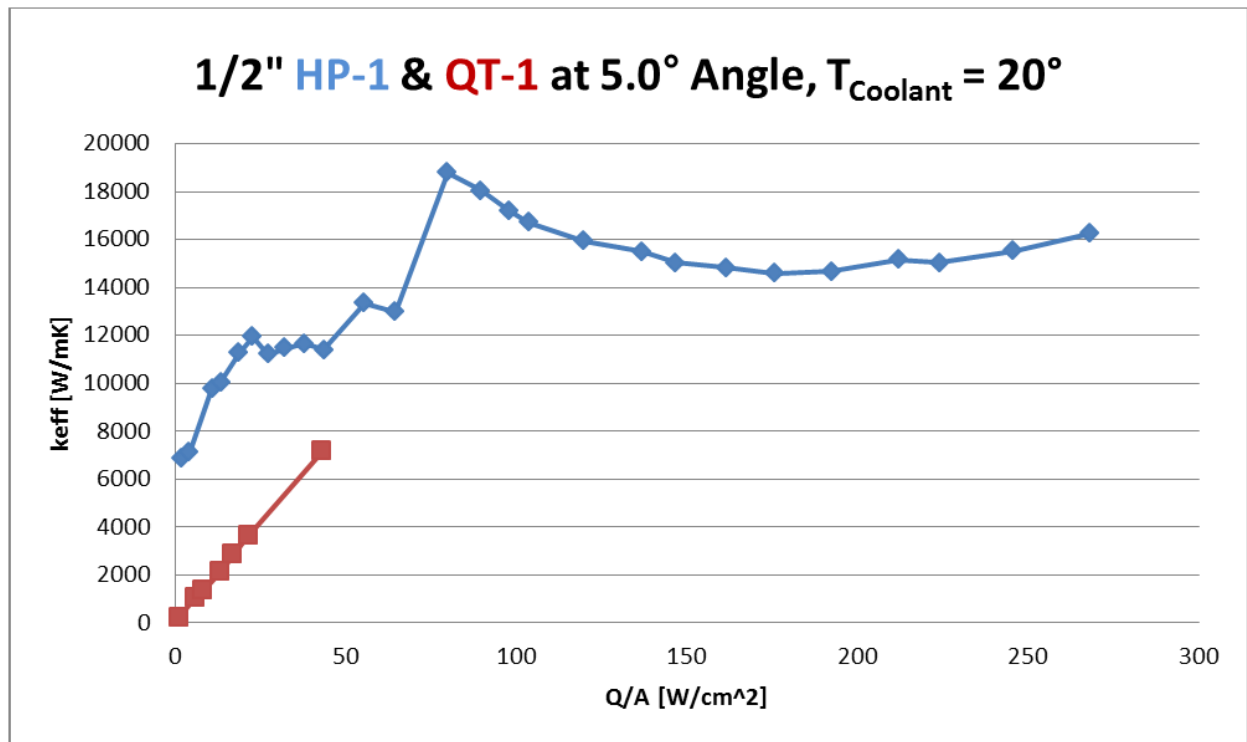


**Figure 26: Effective Thermal Conductivity at Inclination Angle of +5 Degrees (Condenser Upward) and Coolant Temperature of 20°C**

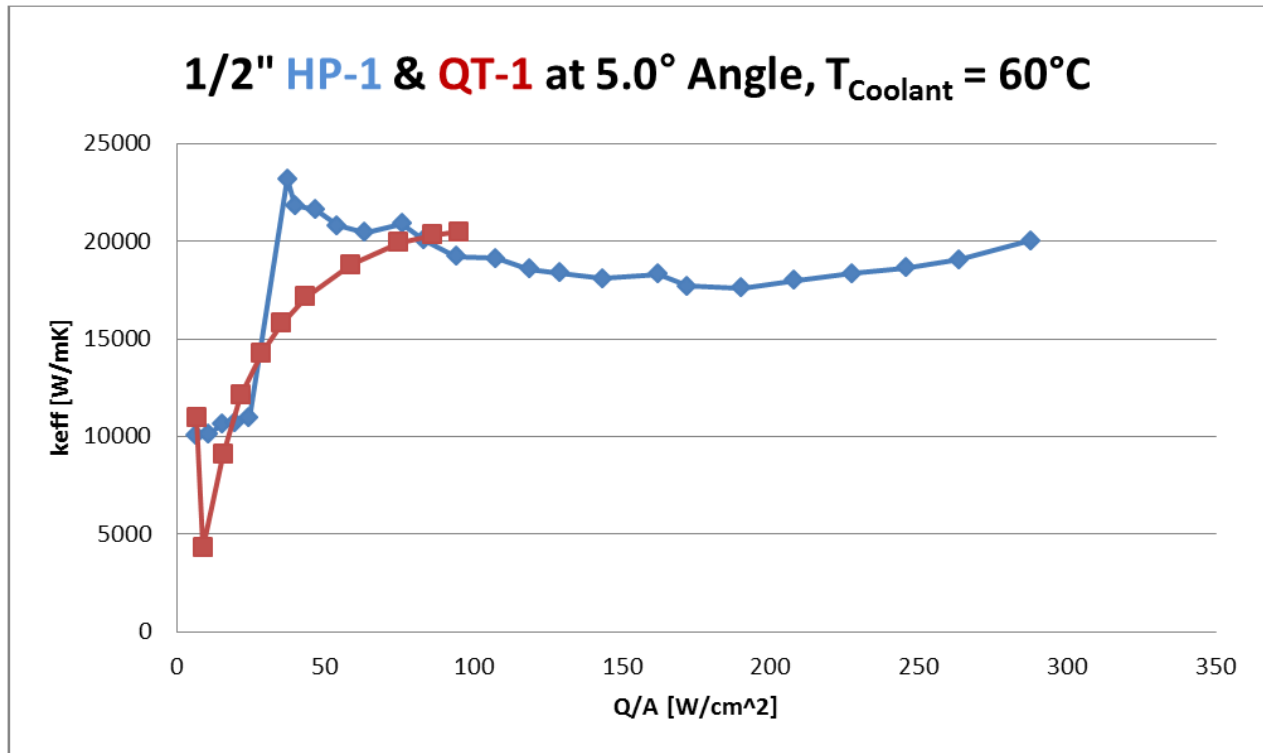


**Figure 27: Effective Thermal Conductivity at Inclination Angle of +5 Degrees (Condenser Upward) and Coolant Temperature of 60°C**

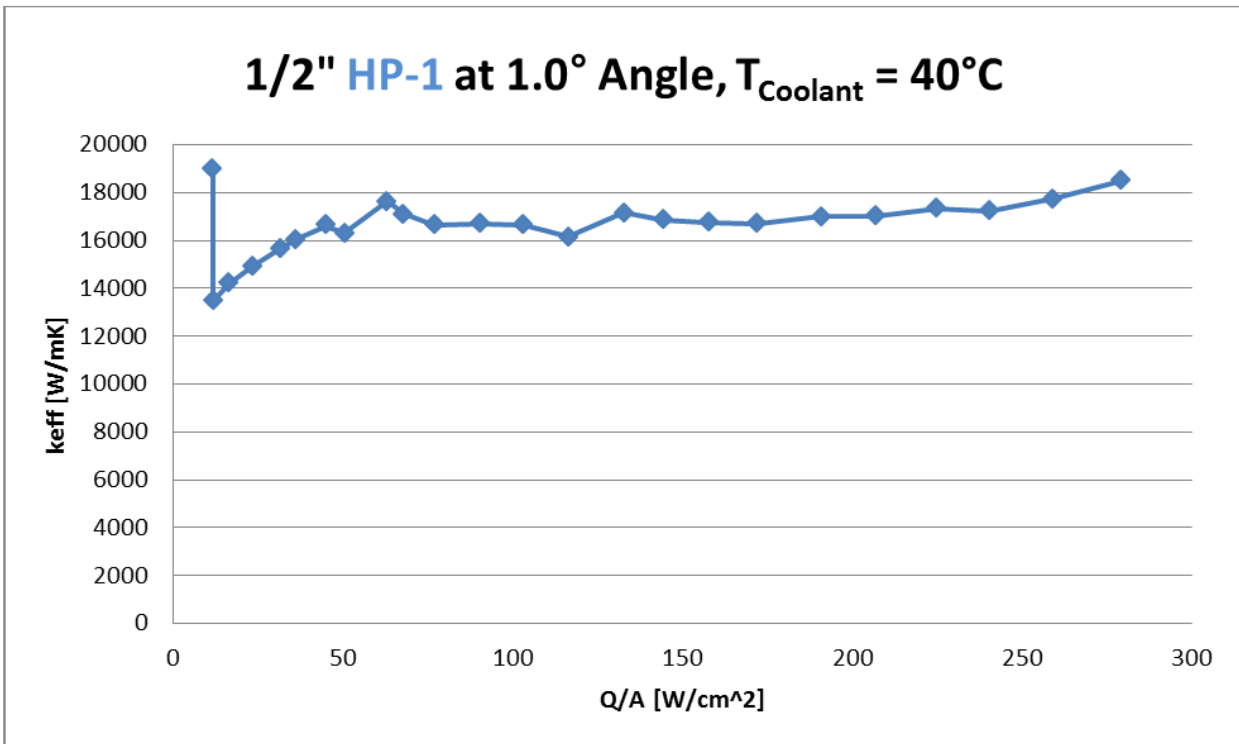


**Figure 28: Effective Thermal Conductivity at Inclination Angle of +1 Degree (Condenser Upward) and Coolant Temperature of 40°C**

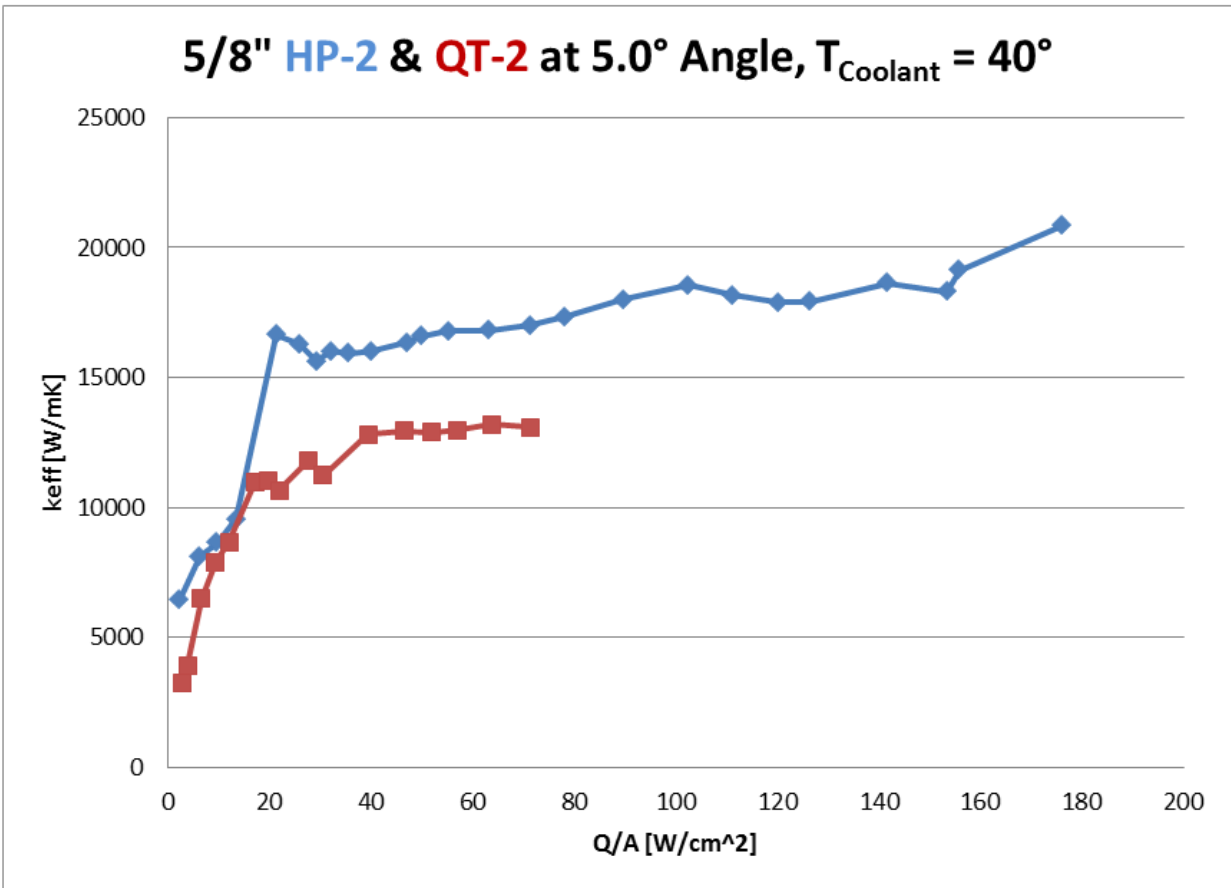


**Figure 29: Effective Thermal Conductivity at Inclination Angle of +5 Degrees (Condenser Upward) and Coolant Temperature of 40°C**

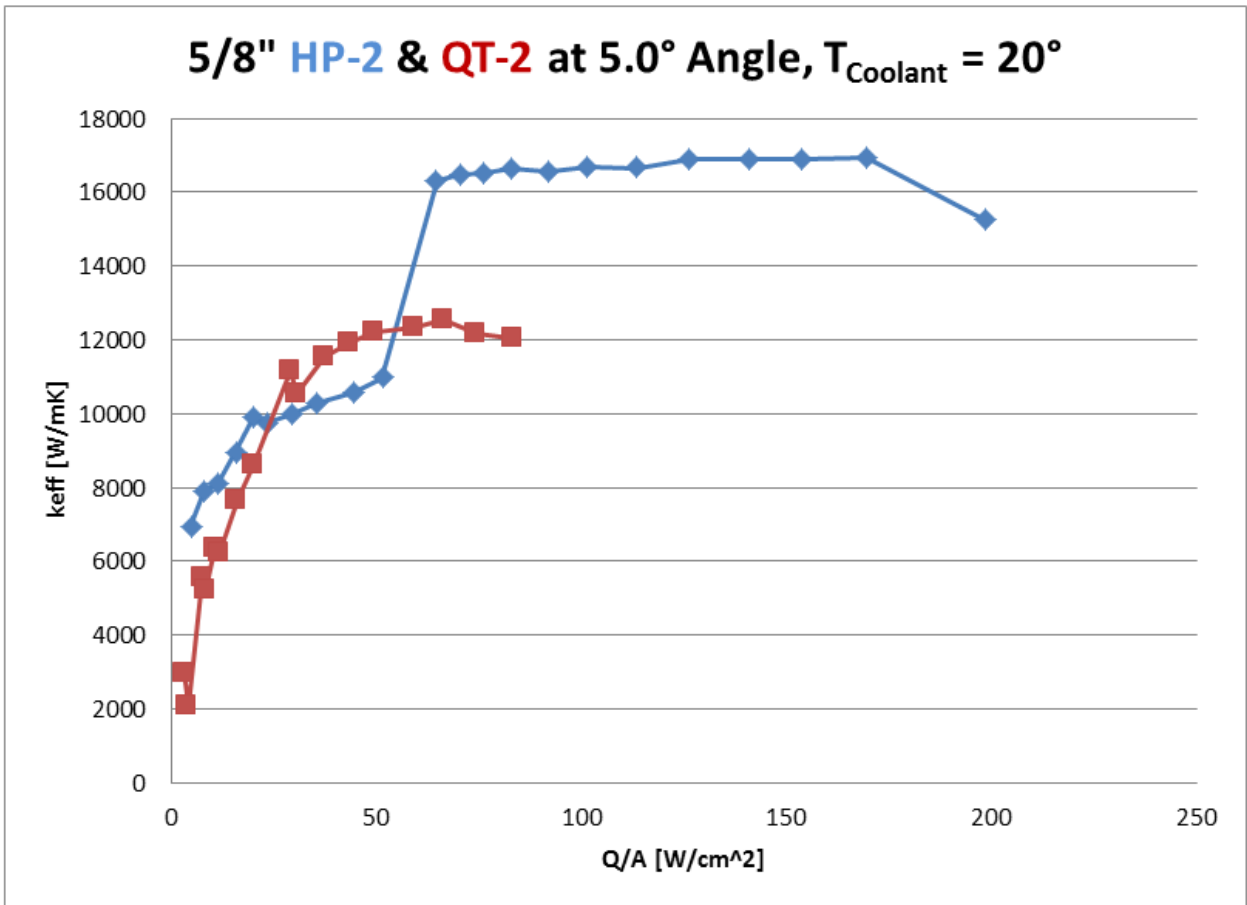


**Figure 30: Effective Thermal Conductivity at Inclination Angle of +5 Degrees (Condenser Upward) and Coolant Temperature of 20°C**

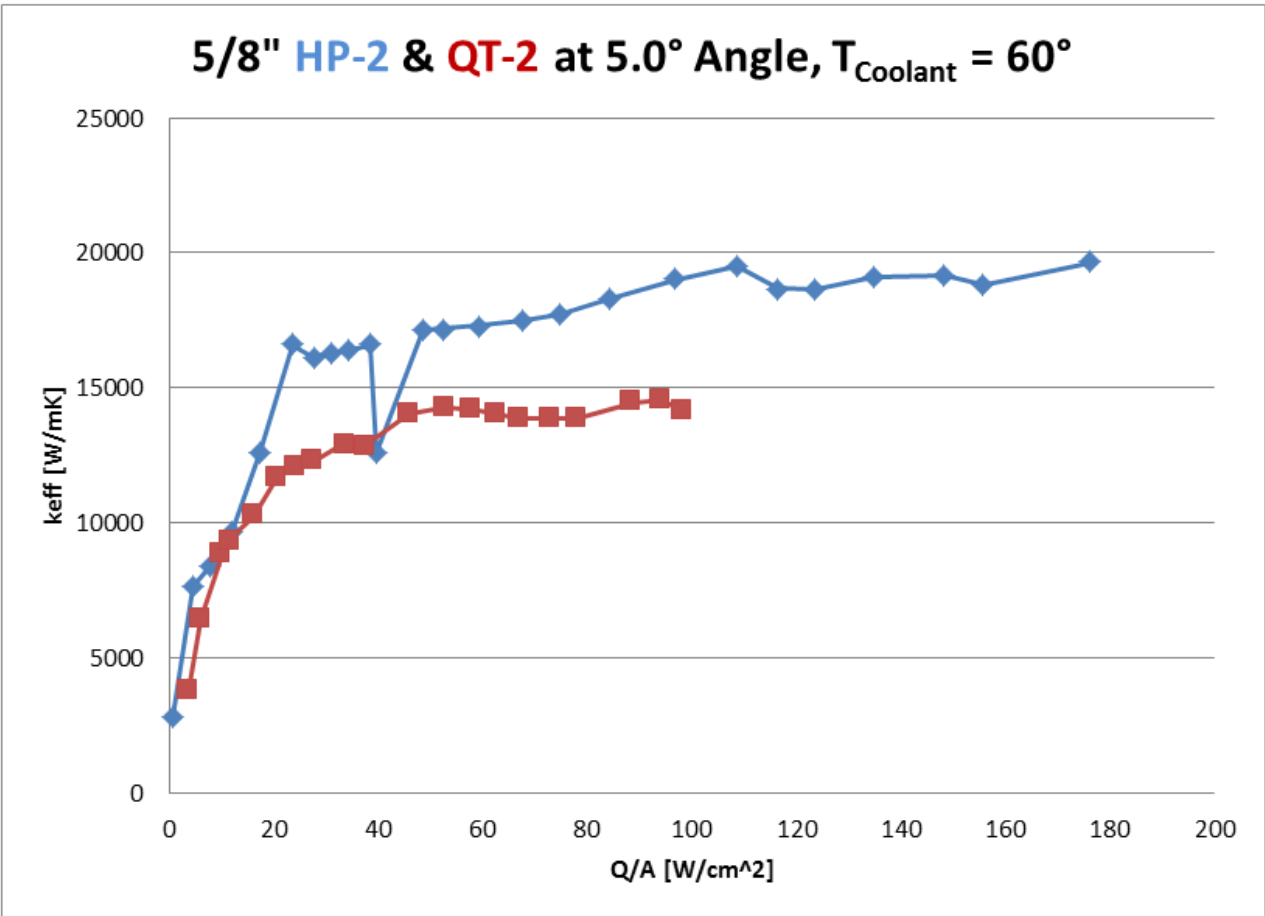


**Figure 31: Effective Thermal Conductivity at Inclination Angle of +5 Degrees (Condenser Upward) and Coolant Temperature of 60°C**

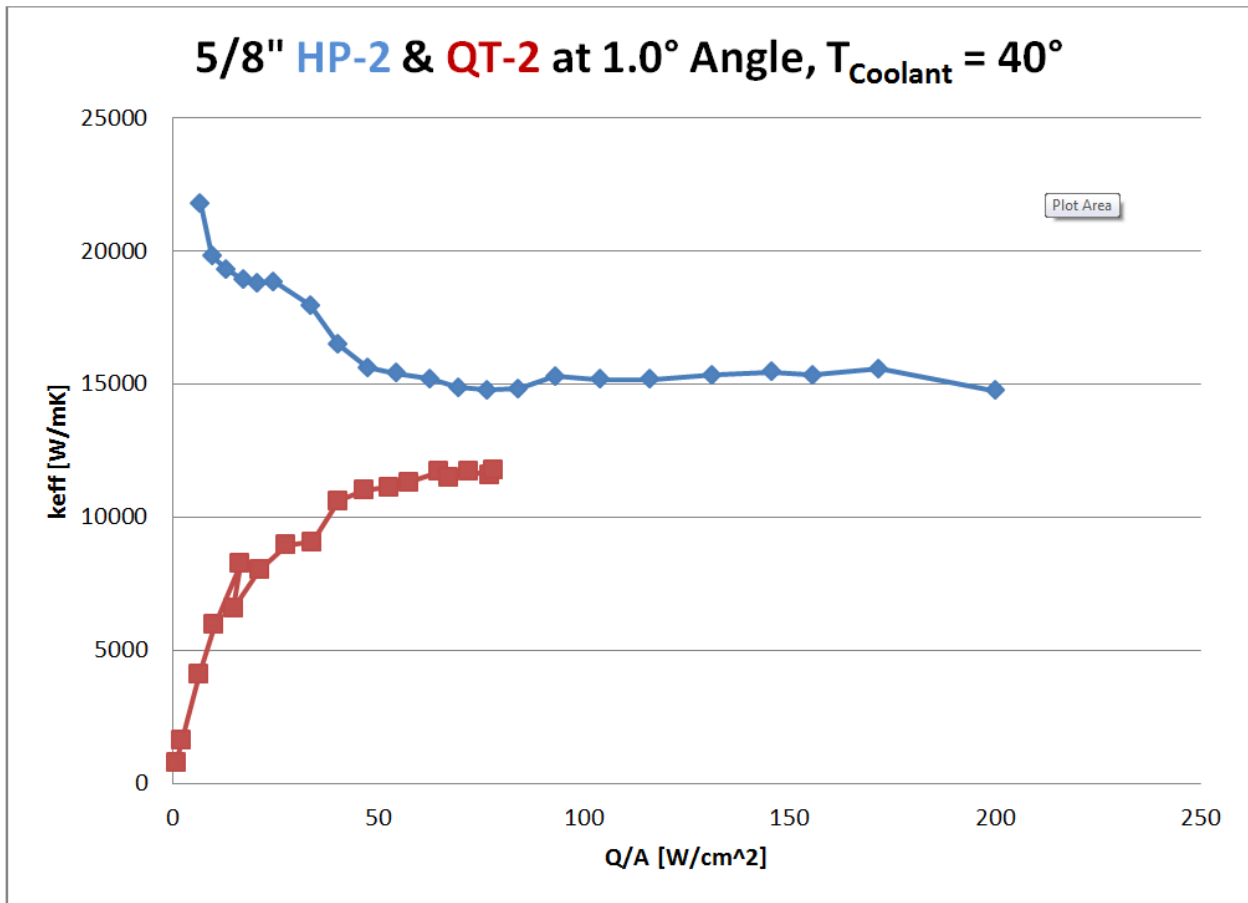


**Figure 32: Effective Thermal Conductivity at Inclination Angle of +1 Degree (Condenser Upward) and Coolant Temperature of 40°C**

## 5.0 CONCLUSIONS AND RECOMMENDATIONS

Both qualitative and quantitative investigations were conducted to comparatively characterize aqueous solution heat pipe transport for four test articles, all 36-inches in length: two Qu-tubes with two different diameters (1/2 in. and 5/8 in.) and two wicked heat pipes with two different diameters (1/2 in. and 5/8 in.). The X-ray imagery revealed the inside state of the test articles, while the IR thermography provided qualitative information on the surface temperature profile developments. The environmentally controlled test, which used a sophisticated LabView DAQ system, allowed for detailed and quantitative characterization of both the Qu-tubes and the wicked heat pipes.

These investigations reveal some fundamental discoveries on the comparative cooling effectiveness between the tested Qu-tubes (Posnett Corp.) and the capillary-pumped heat pipes (Thermacore Inc.):

1. The X-ray imagery of the Qu-tubes show “meniscus-like” interfaces formed by unknown working fluid materials that occupy approximately 10% of the tube length. This observation seriously challenges the inventor’s claim of entirely dry operations on the inside.
2. The Qu-tubes respond more rapidly to heat input during start-up, while the wicked heat pipes tend to provide more stable operations after the initial start-up. The Qu-tubes, however, seem to operate with more stability than the non-wicked heat pipe, which is subject to the most unstable, fluctuating operations.
3. The qualitative IR thermographic images show that the overall temperature gradients from the evaporator to the condenser of the Qu-tubes are somewhat greater than those of the corresponding heat pipes. This alone suggests less effective cooling operation in the Qu-tubes than in the heat pipes.
4. The quantitative measurements for detailed temperature profiles and heat flux amounts provide evidence that the effective thermal conductivities of the Qu-tubes are lower than the heat pipes’. For the Qu-tubes,  $(k_{\text{eff}})_{\text{Qu-tube}} \leq 15,000 \text{ W/m}\cdot\text{K}$ , whereas for the heat pipes,  $15,000 \text{ W/m}\cdot\text{K} \leq (k_{\text{eff}})_{\text{heat pipe}} \leq 20,000 \text{ W/m}\cdot\text{K}$ . In addition, the measured  $k_{\text{eff}}$  values for the Qu-tubes are far below the inventor’s claim of 3,000,000 W/m·K.
5. The adiabatic section temperatures of the Qu-tubes are consistently higher than those of the heat pipes, given identical heater power input. This also supports the previous finding (4) of relatively less effective cooling of the Qu-tubes, in comparison to the heat pipes.
6. The maximum heater power input to the aluminum Qu-tubes was substantially lower than the maximum allowable heater power input to the Cu heat pipes to ensure prevention of the thermal breaching of aluminum.
7. For the negative tilt (-5 degrees), both the Qu-tubes and the heat pipes exhibit unstable operation with dry-out of the evaporator, even with very low heater power input. This

observation questions the inventor's claim of the Qu-tube's gravity-independent operation.

8. The lack of physical resources and scarcity of valid scientific information about the Qu-tubes have prevented us from considering more extensive and comprehensive investigations.

## 6.0 REFERENCES

- [1] Alexander, D. S., *Advanced Energetics for Aeronautical Applications*, NASA/CR-2003-212169, February 2003.
- [2] Blackmon, J. B., and Entekin, S. F., *Preliminary Results of an Experimental Investigation of the Qu Superconducting Heat Pipe*, 2006 Annual Report pp. 12-14, Propulsion Research Center, The University of Alabama in Huntsville, Huntsville, Alabama, 2006.
- [3] Reilly, S., Amouzegar, L., Tao, H. T., and Catton, I., *Use of Inorganic Aqueous Solutions for Passivation of Heat Transfer Devices*, Proceedings 10<sup>th</sup> International Heat Pipe Symposium (IHPS) in Taipei, Taiwan, pp. 153-157, Nov. 6-9, 2011.
- [4] Leland, Q., Ponnappan, R., Lin, L., and Mahefkey, E., *Investigation of Super Tube Structure and Performance*, AFRL Report AFRL-RZ-WP-TP-2011-2078, April 2010.